



## **TRIBOLOGICAL BEHAVIOUR OF PALM OIL BY MIXING FLY ASH MICROPARTICLES AS A BIO-BASED LUBRICANT FOR MACHINING PROCESSES**

Submitted in accordance with the requirement of the Universiti Teknikal Malaysia Melaka (UTeM) for the Bachelor Degree of Manufacturing Engineering (Hons.)



**TAY HOCK SENG**

FACULTY OF MANUFACTURING ENGINEERING  
2021

## DECLARATION

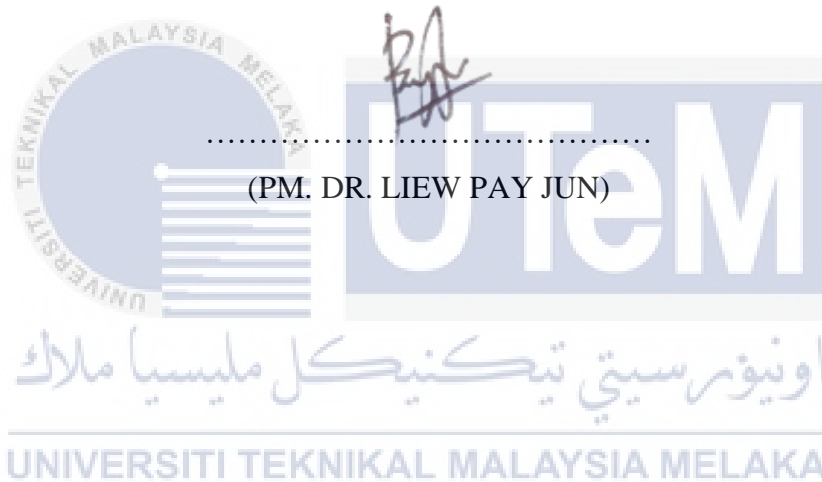
I hereby, declared this report entitled “Tribological Behaviour of Palm Oil by Mixing Fly Ash Microparticles As a Bio-based Lubricant for Machining Processes” is the results of my own research except as cited in reference.

Signature : .....  
Author's Name : TAY HOCK SENG  
Date : 8 February 2021



## APPROVAL

This report is submitted to the Faculty of Manufacturing Engineering of Universiti Teknikal Malaysia Melaka as a partial fulfilment of the requirements for the degree of Bachelor of Manufacturing Engineering (Hons.). The members of the supervisory committee are as follow:



## ABSTRAK

Cecair pelincir digunakan secara meluas semasa proses pemesinan bagi mengurangkan haba yang dijana daripada proses pemotongan. Walau bagaimanapun, terdapat isu bahawa kos cecair pelincir semasa adalah tinggi dan tidak terbiodegradasi. Untuk mengisi jurang penyelidikan, kajian ini bertujuan untuk menghasilkan satu cecair pelincir biodegradasi yang berkos rendah. Objektif kajian ini adalah untuk mengkaji kesan kepekatan zarah-zarah mikro abu terbang yang berbeza dalam bio-pelincir minyak sawit pada pekali geseran, diameter parut kehausan dan permukaan tercalar bola keluli. Dalam penyelidikan ini, pelincir berasaskan bio telah disediakan dengan menyebarkan zarah-zarah mikro abu terbang pada kepekatan 0.02% berat, 0.04% berat, 0.06% berat, 0.08% berat, 0.10% berat, 0.12% berat dan 0.14% berat bersertakan Span 85 sebagai surfaktan dalam minyak sawit dengan menggunakan teknik ultrasonikasi. Ujian tribologikal telah dijalankan dengan menggunakan Tribometer Empat Bola mengikut standard ASTM D 4172. Morfologi permukaan telah dianalisis dengan menggunakan Mikroskop Elektron Imbasan (JEOL6010PLUS). Zarah-zarah mikro abu terbang yang berbentuk sfera didapati telah memberikan kesan menggelek yang paling ketara semasa ujian kehausan sehingga menyebabkan pekali geseran yang paling rendah, diameter parut kehausan yang paling kecil, dan permukaan tercalar yang paling licin pada kepekatan optimum iaitu 0.12% berat.

## ABSTRACT

Liquid lubricants are widely used during machining process to reduce the heat generated from cutting process. However, issue occurs as the current liquid lubricants are high cost and not biodegradable. To fill this research gap, this study aims to produce a low-cost biodegradable liquid lubricant. The objective of this study is to investigate the effect of different concentration of fly ash microparticles in palm oil bio-based lubricant on the coefficient of friction, wear scar diameter and worn surfaces of steel ball. In this research, bio-based lubricants were prepared by dispersing fly ash microparticles at 0.02 wt.%, 0.04 wt.%, 0.06 wt.%, 0.08 wt.%, 0.10 wt.%, 0.12 wt.% and 0.14 wt.% concentrations and Span 85 was used as surfactant in palm oil using ultrasonication technique. The tribological test was conducted using Four Ball Tribometer according to the ASTM D 4172 standard. The surface morphology was analysed using Scanning Electron Microscopy (JEOL6010PLUS). The spherical shape of fly ash microparticles was found to provide most significant rolling effect during wear test that caused lowest coefficient of friction, smallest wear scar diameter and smoothest worn surface in optimum concentration which is at 0.12 wt.%.

## DEDICATION

Only

my beloved father, Tay Peng Swee

my appreciated mother, Cheong Seck Neo

my adored sister and brother, Tay Chai Lian, Tay Hock Lye and Tay Chai Hua

for giving me moral support, money, cooperation, encouragement and also understandings

Thank You So Much & Love You All Forever



## ACKNOWLEDGEMENT

I wish to express my sincere gratitude to my respected supervisor, PM. Dr. Liew Pay Jun for the kindness, unwavering patience and great mentoring that was given to me to complete the project.

I would like to give a thousand thanks to Wong Kah Yan, Yap Ching Yee, and Maisarah binti Kursus as my senior under supervision of PM. Dr. Liew Pay Jun for their willingness to hear my problems and give suggestions during the period of final year project. Last but not least, I would like to give a special thanks to all my best friends who gave me much motivation and cooperation mentally in completing this report.

Finally, I would like to thank everybody who was important to this final year project report, as well as expressing my apology that I could not mention personally each one of you.

UNIVERSITI TEKNIKAL MALAYSIA MELAKA

# TABLE OF CONTENT

Abstrak	i
Abstract	ii
Dedication	iii
Acknowledgement	iv
Table of Contents	v
List of Tables	viii
List of Figures	ix
List of Abbreviations	xi
List of Symbols	xiii

## CHAPTER 1: INTRODUCTION

1.1	Background of Study	1
1.2	Problem Statement	2
1.3	Objectives	3
1.4	Scope	4
1.5	Significant of Study	4
1.6	Organization of Report	5

## CHAPTER 2: LITERATURE REVIEW

2.1	K-Chart	6
2.2	Classification of Lubricant	7
	2.2.1 Solid lubricant	7
	2.2.2 Semi-solid lubricant	9
	2.2.3 Gas lubricant	9
	2.2.4 Liquid lubricant	10
	2.2.4.1 Mineral based oil	10
	2.2.4.2 Synthetic oil	11
	2.2.4.3 Bio-based oil	12
2.3	Tribological & Rheological Behaviour	14



2.3.1	Coefficient of friction	17
2.3.2	Wear	20
2.3.3	Viscosity	21
2.4	Surface Morphology	23
2.4.1	Worn surface	24
2.4.2	Surface roughness	25
2.4.3	Wear scar diameter	26
2.5	Additive Materials	28
2.5.1	Fly ash	33
2.5.1.1	Elements of fly ash	34
2.5.1.2	Properties of fly ash	36
2.5.1.3	Application of fly ash	37
2.6	Parameters	38
<b>CHAPTER 3: METHODOLOGY</b>		
3.1	Materials Selection	42
3.1.1	Characterization of fly ash	42
3.1.2	Palm oil	43
3.2	Preparation of Bio-Based Lubricant	44
3.3	Tribological Test	45
3.4	Surface Morphology Observation	48
<b>CHAPTER 4: RESULTS AND DISCUSSION</b>		
4.1	Tribological Properties of Bio-Based Lubricants	50
4.1.1	Coefficient of friction of steel ball on different fly ash microparticles concentrations	50
4.1.2	Wear scar diameter of steel ball	52
4.2	Surface Morphology Analysis of Steel Ball	54
4.3.2	Observation by SEM	54
<b>CHAPTER 5: CONCLUSIONS AND RECOMMENDATIONS</b>		
5.1	Conclusions	57
5.2	Recommendations	58
5.3	Sustainability Element	58

5.4	Lifelong Learning and Basic Entrepreneurship Element	58
5.5	Complexity Element	59
<b>REFERENCES</b>		60



## LIST OF TABLES

2.1	Examples of hard and soft solid lubricant coatings	8
2.2	Examples of mineral hydrocarbons and their viscosity, molecular mass and carbon number at 5% distillation point	10
2.3	Characteristics of synthetic and vegetable-based base oil	11
2.4	Applications of synthetic lubricant categories	12
2.5	Modification methods on vegetable oils	13
2.6	Parameters of Four Ball Tester used by the 5 studies	16
2.7	Coefficient of friction of additives mixed with base oils at different concentrations	18
2.8	Wear reduction of base lubricants with additives	21
2.9	Viscosity of base lubricant with additives	23
2.10	Surface roughness obtained by other researchers	26
2.11	General types of additives	29
2.12	Different types of additives mixed with different types of base oil	31
2.13	Physical properties of fly ash	37
2.14	Comparison between two lubricants on the coefficient of friction	38
3.1	Chemical composition of fly ash microparticles	43
3.2	Properties of Malaysia palm oil	44
3.3	Lubricants produced with different concentrations of fly ash and palm oil	45
3.4	Parameter used to run Four Ball Tribometer	47
3.5	Wear Scar Diameter	49
4.1	Coefficient of friction	50
4.2	Wear scar diameter	53

## LIST OF FIGURES

2.1	Structure of K-chart research flow	6
2.2	Layered lattice crystal structures of (a) molybdenum disulfide, (b) graphite and (c) hexagonal boron nitride	8
2.3	Friction, wear and lubrication takes place when two surfaces in contact to each other	14
2.4	Pin-on-disk tribometer	15
2.5	Ball-on-disk tribometer	15
2.6	Diagram of Four Ball Tester	16
2.7	Dynamic viscosity of nano-green cutting fluid with MoS <sub>2</sub>	23
2.8	Dynamic viscosity of nano-green cutting fluid with CaF <sub>2</sub>	23
2.9	Morphology of worn surfaces produced during wear tests with (a) sunflower oil, (b) 26 sunflower oil with SiO <sub>2</sub> nanoparticles at 1.25 wt.% and (c) sunflower oil with TiO <sub>2</sub> nanoparticles at 1.0 wt.%	25
2.10	Surface roughness obtained by using different cutting fluid	26
2.11	Wear scar diameter with temperature for different concentration of biodiesel	27
2.12	Optical micrograph of wear scar diameter: (a) pure neem oil, (b) 0.25% GNPs-NO, (c) 0.50% GNPs-NO, (d) 0.75% GNPs-NO and (e) 1.0% GNPs-NO	28
2.13	Wear scar diameter for variety of particle size	31
2.14	Friction coefficient against CNTs concentration	31
2.15	Fly ash	33
2.16	Chemical composition of fly ashes: Major and minor elements	34
2.17	Chemical composition of fly ashes: Class C fly ash and Class F fly ash	35
3.1	Research flow chart	41
3.2	Particle size analysis (Malvern Mastersizer 2000)	42
3.3	X-Ray diffractometer (PANalytical X'Pert Pro)	42
3.4	SEM image of fly ash microparticles	43

3.5	Ultrasonic homogenizer	45
3.6	Four ball tribometer	47
3.7	Schematic diagram of four ball tribometer	47
3.8	Scanning Electron Microscopy (JEOL6010PLUS)	48
3.9	3D Non-contact Optical Profilometer	49
4.1	Coefficient of friction	51
4.2	Schematic diagram of lubrication mechanism	51
4.3	Wear scar diameter	54
4.4	SEM image of worn surface on steel balls	55



## LIST OF ABBREVIATIONS

Ag	-	Silver
AISI	-	American Iron and Steel Institute
Al <sub>2</sub> O <sub>3</sub>	-	Aluminium oxide
ASEM	-	Automated Scanning Electron Microscope
ASTM	-	American Society for Testing and Materials
CaF <sub>2</sub>	-	Calcium Fluoride
CaO	-	Calcium Oxide
CNTs	-	Carbon Nanotubes
Cu	-	Copper
Fe <sub>2</sub> O <sub>3</sub>	-	Iron (III) Oxide
GCFs	-	Green Cutting Fluids
GNPs	-	Graphene Nanoplatelets
hBN	-	Hexagonal Boron Nitride
JMG	-	Jabatan Mineral dan Geosains Malaysia
K <sub>2</sub> O	-	Potassium Oxide
LOI	-	Loss on Ignition
MDD	-	Maximum Dry Density
MgO	-	Magnesium Oxide
MoS <sub>2</sub>	-	Molybdenum disulfide
Na <sub>2</sub> O	-	Sodium Oxide
OMC	-	Optimum Moisture Content
PAG	-	Polyglycols
PAO	-	Poly-alpha-olefin
PI	-	Plasticity Index
POFA	-	Palm Oil Fly Ash
P <sub>2</sub> O <sub>5</sub>	-	Phosphorus Pentoxide
XRD	-	X-Ray Diffractometer
SE	-	Synthetic Ester
SEM	-	Scanning Electron Microscopy

SiO <sub>2</sub>	-	Silicon Dioxide
SO <sub>3</sub>	-	Sulfur Trioxide
SrO	-	Strontium Oxide
TiO <sub>2</sub>	-	Titanium Dioxide
WS <sub>2</sub>	-	Tungsten Disulfide
XRF	-	X-Ray Fluorescence
ZDP	-	Zinc Dithiophosphate



## LIST OF SYMBOLS

%	-	Percentage
wt	-	Weight
°C	-	Degree Celcius
kPa	-	Kilopascal
GPa	-	Gigapascal
Vol	-	Volume
nm	-	Nanometer
µm	-	Micrometer
cP	-	Centipoise
cm/sec	-	Centimeter per second
N	-	Newton
RPM	-	Revolution per minute
kJ/kg°C	-	Kilojoule per kilogram-degree Celcius
kg/m <sup>3</sup>	-	Kilogram per meter cube
W/m°C	-	Watts per meter-degree Celcius

UNIVERSITI TEKNIKAL MALAYSIA MELAKA



# CHAPTER 1

## INTRODUCTION

### 1.1 Background of Study

Lubricant is a substance that is applied in between two moving surfaces to reduce friction, heat and wear. Currently, the most common lubricants in the market are the mineral oils (Abdollah et al., 2020). This is due to its low cost and good tribological performance. However, these mineral oils demonstrated a destructive environmental effect because they are not biodegradable and harmful. This will further lead to a higher cost in waste management. Furthermore, there is increasing concern on the use of these mineral oil lubricants on environmental impact as they were consumed about 38 million metric tons worldwide (Abdollah et al., 2020).

Nowadays, strict environmental regulations have forced the market to move toward bio-based lubricants because of their biodegradable properties. Not only that, bio-based lubricant or specifically vegetable oils have many good properties such as low volatility, high viscosity, low toxicity, high flash point and high lubricity. The most common types of vegetable oils used as lubricants that currently being researched on are sunflower oil, neem oil, jatropha oil and coconut oil. However, researchers have not treated palm oil in much detail. Therefore, palm oil will be used as base oil in this study. Abdollah et al. (2020) stated that palm oils produced a higher wear rate than mineral oils due to its incomplete oxidation and thermal stability, solidified at low temperature and low viscosity. Although these are the disadvantages of palm oil other than the environmental advantages, it can be fixed by mixing up with additive materials through process called ultrasonication.

The physical properties of the lubricant such as wear and corrosion can be intensified by introducing additive materials into the lubricant (Chan et al., 2018). The aim is to have a

longer tool life span, less coefficient of friction and better performance on machining process. The most commonly used additive materials in the lubricants are graphite, molybdenum disulfide, tungsten disulfide ( $WS_2$ ), ester and zinc dithiophosphate (ZDP) (Kopeliovich, 2012). Fly ash is a by-product of coal thermal power plants. Hower et al. (2017) has predicted that about 750 million ton of coal ash are generated all over the world annually. Fly ash can cause environmental pollution if does not dispose properly. Therefore, efforts have been made to recycle fly ash and thus fly ash is extensively used in concrete and ceramic industry due to its large surface area. Although extensive research has been carried out on applications of fly ash, however, the application of fly ash as additive materials in lubricant is still scarce. Therefore, in this study, fly ash will be used as the additive material that will be mixed into palm oil to become an environmental-friendly lubricant. The effect of fly ash microparticles mixed into palm oil on the tribological behaviour especially on the coefficient of friction and wear will be investigated.

## 1.2 Problem Statement

Machining is one of the most crucial processes in the manufacturing industry which involve the removal of materials from the stock or billet with a cutting tool. In machining operation, the removal of materials from the workpiece only used about 40% of energy (Astakhov, 2006). The other 60% of energy is used at the tool-chip and tool-workpiece interfaces. Tool-chip and tool-workpiece interfaces are the contacts areas that directly involved in the cutting process. Furthermore, all the energy spent during cutting process will be converted into heat energy (Bhirud and Gawande, 2017). When machining low strength alloys, less heat is generated but high heat will be generated when high strength alloys are machined due to increasing in cutting speed. The generated heat, if does not dissipate successfully, will affect the wear rate of cutting tool thus affecting the surface finished quality (Ogedengbe et al., 2019).

Many techniques were introduced to help in reducing the heat generated from the cutting process. One of the techniques is by using lubricant during the machining process. There are a few types of lubricant such as solid, liquid, semi-solid and gas lubricant. Liquid lubricant contains bio-based oil such as sunflower oil, neem oil and coconut oil. The tribological behaviour of these oils in machining processes are currently being researched

by many researchers. However, there has been little quantitative analysis of palm oil as lubricant for machining process. Palm oil is known for its immeasurably proficient yield, which create more oil per land ratio than other vegetable oil crop such as soybean oil or coconut oil (Abdollah et al., 2020). Not only that, palm oil as lubricants exhibits great tribological properties when mixed with additive materials.

Additive materials or lubricant additives are chemical components that helps to improve the physical properties of a lubricant in machining process (Corporation, 2018). At present, oil mixed with additive materials such as graphite, graphene nanoplatelets (GNPs), molybdenum disulfide, tungsten disulfide ( $WS_2$ ), ester and zinc dithiophosphate (ZDP) are widely used as lubricant for machining process (Kopeliovich, 2012). Although these additive materials helped in reducing coefficient of friction and wear rate of cutting tools, but they are expensive (Cao and Xia, 2017). Therefore, attentions are now centred to fly ash. Fly ash is cheap and it also exhibits certain excellent properties such as low coefficient friction and low wear rate when integrated in automotive brake lining friction composites (Mohanty and Chugh, 2007). Furthermore, fly ash is widely available as it is a by-product produced from the combustion of pulverized coal.

Currently, annual world production of fly ash is predicted to be over 500 million tonnes where only less than 20% of it is recycled and used as pozzolan to produce cement (Amran et al., 2020). The rest is disposed of in landfills and ash ponds. This will lead to environment pollution where the toxic compounds leach into underground waterbed. Therefore, the study of tribological behaviour of fly ash microparticles mixed with palm oil as an environment friendly lubricant needs to be done to reduce the effect of environment pollution.

### **1.3 Objectives**

The purpose of this study is to investigate the tribological behaviour of palm oil by mixing fly ash microparticles as a bio-based lubricant for machining process. Detailed objectives of this study are as follows:

1. To investigate the tribological performance (coefficient of friction and wear) of the palm oil blended with fly ash microparticles.
2. To investigate the surface morphology of worn surfaces on the steel balls after the tribological test.

#### **1.4 Scope**

To achieve the objectives, few scopes are set as shown below:

1. Producing an environment-friendly lubricant using palm oil and fly ash microparticles as additives.
2. Mixing palm oil and fly ash microparticles of concentration ranging between 0.02 and 0.14 wt.% using ultrasonic homogenizer.
3. Testing the tribological behaviour of environment-friendly lubricant using Four Ball Tester (ASTM D 4172).
4. Observing surface morphology of worn surfaces using 3D non-contact optical profilometer and scanning electron microscopy (SEM).

#### **1.5 Significant of Study**

There are some benefits that can be obtained when this study is completed. First is the production of bio-based lubricant which is an environment-friendly lubricant that means it does not have or produce less impact on the environment pollution when being disposed of. Next, the cost of producing this lubricant will be reduced due to the use of fly ash as recycle materials. This is because fly ash is abundant, can be obtained easily and 60% of them in the world is not being recycled.

## 1.6 Organization of Report

The overall organization of the study took the form of five chapters, including this introductory chapter. Chapter 1 discussed on the background of study and the problems that were identified through multiple researches of journals, articles and current news. It was then followed by objectives that were set to be achieved through scope which narrowed down the area of the study. The significant of the study to the machining industry was also disclosed.

Chapter 2 began by reviewing the classifications of lubricants and followed by the types of oil available in each lubricant. It was then continued reviewing on the types of vegetable oils that people normally researched on. After that, definition of additive materials and the most common additives materials that were being used as lubricant additives was mentioned. Not only that, the additive material that were used in this study were also discussed. Lastly, the methods for experimenting the lubricants and the parameters were described.

Chapter 3 described the methods and procedures to achieve the objectives mentioned in this study. The flow started from explaining the materials used to the methods used to mix up the materials into lubricant. This was followed by the analysis or experiments to determine the tribological behaviour of bio-based lubricant and the surface morphology of worn surface produced on the steel ball.

Chapter 4 analysed the information and data collected after conducting tribological behaviour of bio-based lubricant through Four Ball Tester. Then, the surface morphology of worn surface of the steel ball were also observed and discussed in this chapter.

Chapter 5 summarized the tribological behaviour of the fly ash microparticles mixed with palm oil as an environment-friendly lubricant.

## CHAPTER 2

### LITERATURE REVIEW

#### 2.1 K-Chart

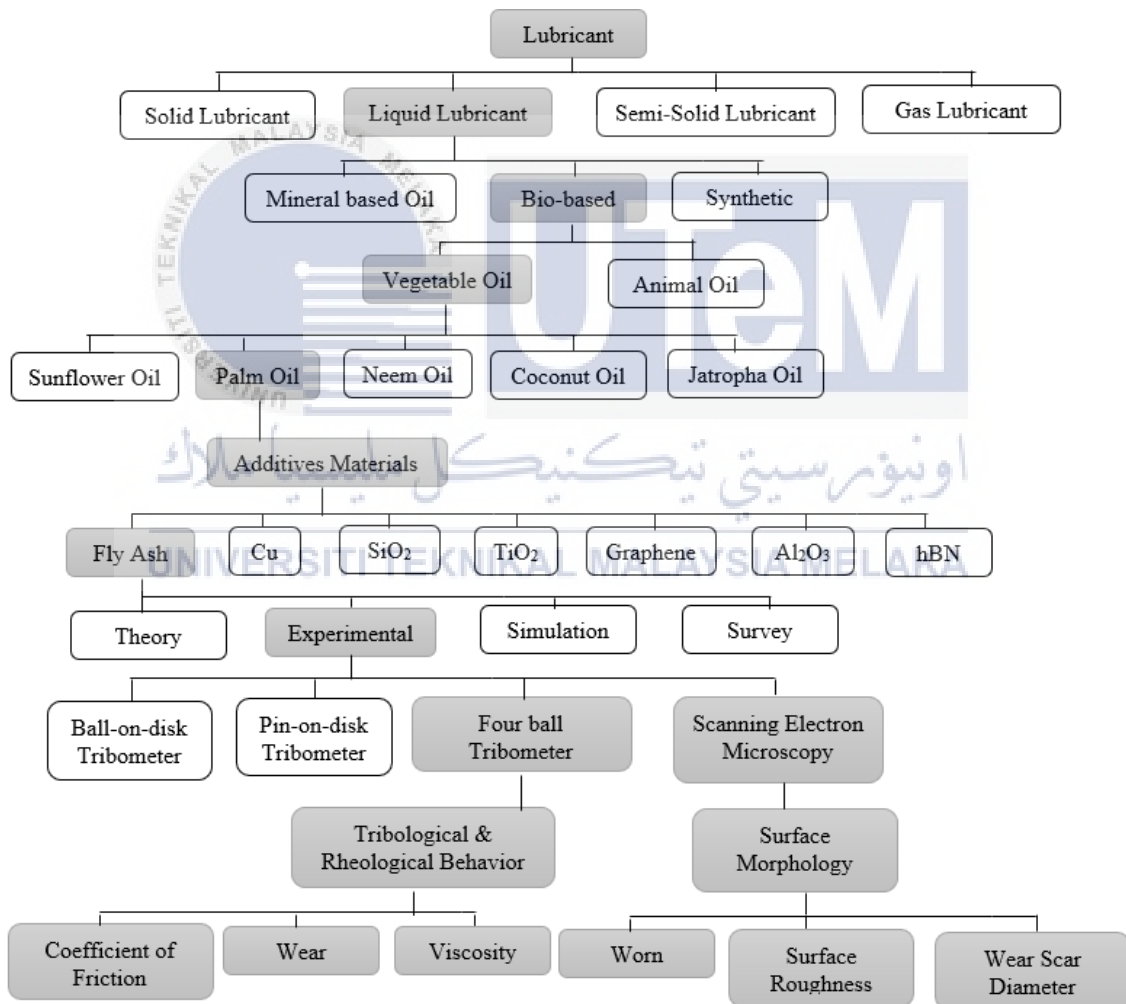


Figure 2.1: Structure of K-chart research flow

Figure 2.1 shows the structure of K-chart research flow for this study. K-chart is a tool that organizes the problems from the general ones to the specific ones within the area under study. K-chart consists of general title, issues layer, methods layer, results layer and

timeline in the form of a tree diagram. The development of K-chart structure bases on the researcher requirement to achieve the objective in the study (Khazani et al., 2006). In this study, K-chart was developed to be used in this chapter and the next chapter, methodology.

## 2.2 Classification of Lubricant

Lubricant is an element that is used in between two surfaces to reduce friction, wear and tear. In machining processes, lubricants are used for heat transfer, lubrication and corrosion protection. In a high-level grouping of products, lubricant plays an important role in industry and transportation because there will be no energy transfer if no lubrication is available. According to Bart et al. (2013a), lubricants is classified into 4 groups which are solids, semi-solids, gas and liquids.

### 2.2.1 Solid lubricant

Solid lubricant is a material that able to reduce friction between two moving surfaces without requiring any other liquid substances. It is a material in the solid form. Bart et al. (2013a) mentioned in the article that solid lubricant is used as coating which can provide surfaces from being damaged by decreasing the friction, wear and tear of the two contacting surfaces. In another source, Bart et al. (2013b) stated that these solid lubricants are made up of solid, binder and additives. Solid lubricants are used during important cases where the lubricants had to stay in place. Usually have a temperature range where they are highly effective, these solid lubricants may degrade if they reach above their optimum temperature. For example, graphite as solid lubricants able to withstand temperature up to 650°C before they start to degrade physically and chemically. According to Donnet and Erdemir (2006) and Campañá and Müser (2007), example of generally used solid lubricants are graphite, molybdenum disulfide, hexagonal boron nitride, boric acid and tungsten disulfide. Most of the solid lubricants have unique lubricating properties because they are associated with layered lattice crystal structure as shown in Figure 2.2.

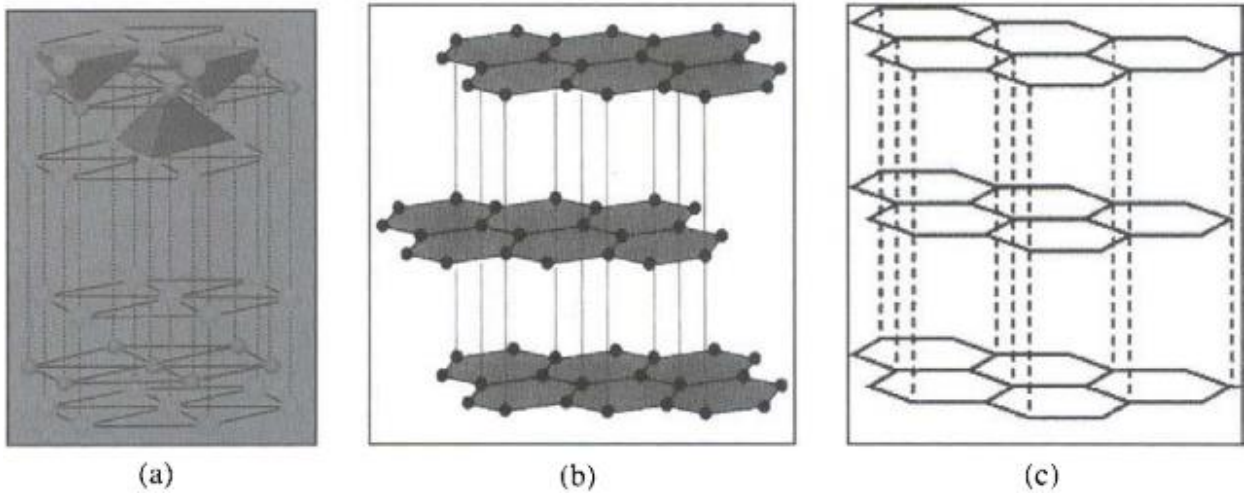


Figure 2.2: Layered lattice crystal structures of (a) molybdenum disulfide, (b) graphite and (c) hexagonal boron nitride (Donnet and Erdemir, 2006).

Solid based coating can be categorized into 2 main groups: Soft solid lubricant coating (below 10GPa hardness) and hard solid lubricant coating (above 10GPa hardness). It is categorized based on their chemical, physical, mechanical and structural properties. Table 2.1 shows some examples of soft and hard solid lubricant coatings. Soft solid lubricants can produce low friction with low wear resistance while hard solid lubricants can produce low friction with higher wear resistance than soft solid lubricants (Donnet and Erdemir, 2006).

Table 2.1: Examples of hard and soft solid lubricant coatings (Donnet and Erdemir, 2006)

<b>Hard solid lubricant coatings</b> Hardness higher than $\approx 10\text{Gpa}$	<b>Soft solid lubricant coatings</b> Hardness lower than $\approx 10\text{GPa}$
<b>Nitrides</b> CBN, $\text{CN}_x$	<b>Soft metals</b> Ag, Pb, Au, In, Sn, Cr, Ni, Cu
<b>Carbides</b> $\text{TiC}$ , $\text{WC}$ , $\text{CrC}$ , $\text{SiC}$ CDC, $\text{Ti}_3\text{SiC}_2$	<b>Lamellar solids</b> $\text{MoS}_2$ , $\text{WS}_2$ , Graphite $\text{H}_3\text{BO}_3$ , HBN, GaS, GaSe
<b>Oxides</b> $\text{TiO}_2$ , ZnO, CdO, $\text{Cs}_2\text{O}$ , PbO $\text{Re}_2\text{O}_7$	<b>Halides, sulfates, sulfides</b> $\text{CaF}_2$ , $\text{BaF}_2$ , PbS, $\text{CaSO}_4$ , $\text{BaSO}_4$
<b>Borides</b> $\text{TiB}_2$ , $\text{AlMgB}_{14}$	<b>Polymers</b> PTFE, PE, Polyimide Polymerlike DLC (high hydrogen content)
<b>DLC &amp; Diamond</b> a-C, ta-C, a-C:H, ta-C:H a-C:X(:H), (nc-)diamond	<b>Quasicrystals</b> Al-Pd-Mn, Al-Cu-Fe, Al-Ni-Co-Si

DLC = diamondlike carbon

X = a metal

carbon

PTFE = polytetrafluorethylene

a = amorphous

nc = nanocrystalline

PE = polyethylene

ta = tetrahedral amorphous

CDC = carbide derived



### 2.2.2 Semi-solid lubricant

Semi-solid lubricants are substances that are neither liquid nor solid at room temperature. They are prepared by using saponification of fat with alkali which then followed by adding lubricating oil. As stated by Paul and Varadarajan (2013), semi-solid lubricant helps in transferring heat generally in the evaporative mode which was more capable than the traditional heat transfer. The most common semi-solid lubricant used in lubricant application is grease. Grease is composed of sodium, calcium and mineral oil. It is used in application such as bearings, gears and stamping process where high-pressure work is needed. Grease is also used in metal cutting processes where liquid lubricants cannot be maintained. Based on the study done by Paul and Varadarajan (2013), the performance of semi-solid lubricants can be further improved by adding 10% of graphite into the grease. This will produce a result of lower coefficient of friction and lower cutting force than the standard grease.

### 2.2.3 Gas lubricant

According to BARTZ (1974), gas lubricant is a lubricant that has lowest viscosity because it is consist of air, nitrogen, oxygen and helium. In applications that require good dimensional stability and minimum perturbation, gas lubricant serves very well by moving at high speed through small gaps due to its low density and viscosity (Maxwell, 1985). Gas lubricant has few advantages, one of it is that their chemical stability enables them to be used in industry like food, pharmaceutical and electronic industries where contamination is highly judged as important criteria. Furthermore, Lentini et al. (2018) stated that gas lubricant has small range of viscosity changes over a wide range of temperature which is from  $-267^{\circ}\text{C}$  to  $1648^{\circ}\text{C}$ . These properties of gas lubricants cause them to be widely used in aerospace and cryogenic applications. However, gas lubricant has low load-carrying capacity of 15-20kPa due to its low viscosity.

## 2.2.4 Liquid lubricant

Liquid lubricant is a substance that reduces friction and wear in between two moving surfaces by providing a continuous flow of fluid in between them (Yunus and Luo, 2017). They act as a heat transfer, corrosion preventor and sealing agent (Thomas, 2020). Liquid lubricants are usually used in high speed and high load applications. They are mixed with additive materials and classified into 3 main groups depending on the base oil used: Mineral based oil, synthetic oil and bio-based oil.

### 2.2.4.1 Mineral based oil

Mineral oils are oils that are refined from crude oil. It is widely used as engine oils, lubricating oils and processing oils as in rubber industries due to its low extracting cost (Armstrong et. al., 2018). Minerals oils can be produced in wide range of viscosity which makes them very useful in many applications. There are 3 basic types of mineral oil: paraffinic, naphthenic and aromatic (Harvey, 2010). Paraffinic oils are produced by hydrocracking. It is the process whereby hydrocarbon molecules of petroleum are broken down into simpler molecules such as kerosene and gasoline (Chishi, 2018). Paraffinic oils possessed high resistant to oxidation and high flash and fire point. On the other hand, naphthenic oils are made from crude oil distillates. They are sometimes called as pale oils due to their pale in colour. Naphthenic oils have the properties of low viscosity, low flash and fire point and low oxidation resistance and are usually used in the production of power transformer oils (Chishi, 2018). Lastly, aromatic oils are the refined versions of paraffinic oils. They are dark in colour and have high flash and fire point. These aromatic oils are used for softening and plasticizing effect which are in rubber and asphalt production (Aromatic Oils, 2020). Table 2.2 shows some examples of mineral oils with their viscosity, average relative molecular mass and carbon number.

Table 2.2: Examples of mineral hydrocarbons and their viscosity, molecular mass and carbon number at 5% distillation point (Vavasour and Chen, 2003).

Name	ADI (mg/kgbw) <sup>a</sup>	Viscosity at 100°C (mm <sup>2</sup> /s)	Average relative molecular mass	Carbon number at 5% distillation point
Microcrystalline wax	0-20 <sup>a,b</sup>	≥11	≥500	≥25

High-melting-point wax		Not included in present studies		
Low-melting-point wax	Withdrawn <sup>c</sup>	No JECFA specification		
Low-melting-point wax		3.3	380	22
Mineral oil (high viscosity)	0-20 <sup>a</sup>	>11	>500	≥28
P100		11	520	29
Mineral oil (medium and low viscosity)	0-10 <sup>d</sup>	8.5-11	480-500	≥25
Class I				
P70		9.0	480	27
Medium-viscosity liquid petroleum		8.7	480	25
P70(H)		8.6	480	27
Mineral oil (medium and low viscosity)	0-0.01 <sup>e</sup>	7.0-8.5	400-480	≥22
Class II				
N70(H)		7.7	420	23
Mineral oil (medium and low viscosity)	0-0.01 <sup>e</sup>	3.0-7.0	300-400	≥17
Class III				
P15(H)		3.5	350	17
N15(H)		3.5	350	17

#### 2.2.4.2 Synthetic oil

Synthetic oils consisted of oil components that are produced synthetically. According to Bart et al. (2013a), synthetic oils are more remarkable than refined oil in most of the case. Examples are shown in Table 2.3. Synthetic oils have one disadvantage which is they are costlier than mineral oils. Some frequently used synthetic oils are poly-alpha-olefin (PAO), polyglycols (PAG), silicones and synthetic ester (SE). Guzman et al. (2018) mentioned that synthetic ester oil can withstand high temperature and provide good detergency. Table 2.4 shows the applications of synthetic lubricant categories.

Table 2.3: Characteristics of synthetic and vegetable-based base oil (Bart et al., 2013a).

Synthetic	Vegetable-based
<ul style="list-style-type: none"> <li>• Better oxidation stability or resistance</li> <li>• Better VI</li> <li>• Much lower PP (as low as -78°C)</li> <li>• Lower CoF</li> </ul>	<ul style="list-style-type: none"> <li>• Good boundary lubrication</li> <li>• General wear protection</li> <li>• High VI</li> <li>• High flash point</li> <li>• Low volatility</li> </ul>

Table 2.4: Applications of synthetic lubricant categories (Bart et al., 2013a).

Category	Applications
Synthesised hydrocarbon <sup>a</sup>	Engine and turbine oils (incl. transformer oils) Hydraulic fluids Gear and bearing oils Compressor oils (incl. refrigerator oils)
Organic esters <sup>b</sup>	Crankcase oils Compressor lubricants
Phosphate esters	Fire-resistance applications
Polyglycols	Gears Bearings Compressors for hydrocarbon gases
Silicones	Fire-resistance applications Industrial and military installations

<sup>a</sup>E.g. PAOs and dialkylated benzenes.

<sup>b</sup>E.g. dibasic acid and polyol esters.

### 2.2.4.3 Bio-based oil

According to Syahir et al. (2017), bio-based oil is referred to lubricants that gained from vegetable oils and animal fats. They are called bio-based oil because they are biodegradable and renewable. In addition, they are known for their lubricity, flash and fire point, viscosity and resistance to shear when compared to mineral oils. Bio-based oils are divided into two groups: Vegetable oils and animal fats. Animal fats lubricants are produced from animal fats. There are two main animal fats, which are hard fats and soft fats. These animal fats are usually used to manufacture grease. Other than that, Matiliunaite and Paulauskiene (2019) pointed out that animal fats lubricants can also be used in fishery, forestry and agriculture industry because they are biodegradable.

Vegetable oils are extracted from seed, or part of fruits (Konie, 2020). They are environmentally friendly because they are biodegradable. Vegetable oils are an alternative to minerals oils since they carried lubrication properties such as good contact lubrication and high viscosity index (Campanella et al., 2010). The only drawbacks about vegetable oils are their low oxidation and temperature stabilities. To counter this problem, Syahir et al. (2017) mentioned that chemical modification can be done on the vegetable oils to improve the oxidation stability of vegetable oils for a wide range of temperature. Table 2.5 shows the modification methods on vegetable oils and the advantages and disadvantages of each method. Some common examples of vegetable oils that are currently being researched on are sunflower oil, neem oil, coconut oil and jatropha oil.

According to Salah et al. (2017), the coefficient of friction of pure sunflower oil when tested using ball-on-disk tribometer was 0.142. The test was done at the temperature of 100°C. From the study done by Suresha et al. (2020), the coefficient of friction for neem oil tested by Four Ball Tester is 0.118. The test was conducted at temperature of 55°C. From the data, it is known that neem oil is a better vegetable oil as lubricant when compared to sunflower oil. This is because at temperature of 55°C, neem oils were able to produce lower coefficient of friction than sunflower oils at 100°C. In another study, Khan et al. (2019) stated that coconut oil as lubricant has the coefficient of friction of 0.01 at temperature 37.5°C when tested with pin-on-disk tribometer. Another study was done on sunflower oil by Cortes et al. (2020). They found that the coefficient of friction for sunflower oils were at 0.0511 at temperature of 25°C when conducted using block-on-ring tribometer. When compare to the study done by Salah et al. (2017), the sunflower oil doesn't have the same coefficient of friction. The reason is may be that the sunflower oils were gained from different sources. Talib et al. (2017) discussed that crude jatropha oil and modified jatropha oil have the coefficient of friction of 0.052 and 0.023, respectively. Both the oils are tested by using Four Ball Tester at 100°C. Abdollah et al. (2020) has researched on tribological behaviour of palm oil with hexagonal boron nitride and found that pure palm oil has the coefficient of friction of 0.04 at temperature 75°C using Four Ball Tester. All the procedures done using Four Ball Tester were based on the ASTM D 4172 standard.

Table 2.5: Modification methods on vegetable oils (Syahir et al., 2017).

Method	Description	Advantages	Disadvantages
Esterification / transesterification	Transformation of ester into another ester through interchange of alkoxy moiety.	-Improves oxidative stability and low temperature characteristics	-Requires feedstocks with high oleic acid content -High reaction temperature
Estolide formation	Estolides formed either through the addition of a FA to a hydroxyl containing fat or by the condensation of a FA across the olefin functionality of a fat.	-Improves oxidative stability and low temperature characteristics -Low reaction temperature -Can be used on variety of vegetable oils	-Expensive capping FA often needed for the initial reaction
Selective hydrogenation	Reaction between molecular hydrogen atom with another compound or element. Transforms multiple unsaturated FAs into a single FA.	-Reduce the degree of unsaturation -Increase oxidative stability	-Newly formed monoenic acids can isomerize to form cis-acids and trans-acids that can alter end product's properties significantly. -High reaction temperature

Epoxidation	Introduction of a new epoxide functional group (cyclic ether) resulted from the double bond removal between two carbon atoms, via an oxygen atom.	-Improves lubricity and oxidative stability -Low reaction temperature	-Increases pour point value -Decreases viscosity index
Additional ring opening and / or acetylation after epoxidation	Ring opening: Introduction of hydroxyl group from the cleavage of carbon-oxygen bonds. Acetylation: Conversion of hydroxyl group present in vegetable oils into acetate.	-Produces final product with ideal lubricant properties	-High production cost

### 2.3 Tribological & Rheological Behaviour

Tribology is the study of interacting two surfaces in motion that relates to their friction, wear, lubrication and design (Das, 2019; Niraj et al., 2018). In the book published by Nosonovsky et al. (2013), tribology came from the word *tribos* which meant the science of collaborating surfaces in corresponding motion or rubbing process. It discusses on what happens when two materials rub together. Figure 2.3 shows tribological behaviour of two contacting surfaces.



Figure 2.3: Friction, wear and lubrication takes place when two surfaces in contact to each other (Karpinska, 2016).

There are few experiments generally used by researcher to conduct the study of tribological behaviour on lubricants. The examples are ball-on-disk tribometer, pin-on-disk tribometer and Four Ball Tester. All these tests were used to investigate the friction and wear

of lubricants. Ball-on-disk and pin-on-disk tribometer have almost similar setup, the difference is that ball-on-disk use ball to contact with the surface while pin-on-disk use pin. Figure 2.4 and Figure 2.5 show the difference between pin-on-disk and ball-on-disk tribometer. Both use ASTM G99 standard for the test to determine the coefficient of friction, wear track, wear rates, wear resistance, wear scar diameter and wear volume of by putting a variety of load on the ball or pin with a range of sliding speed at a fixed duration.

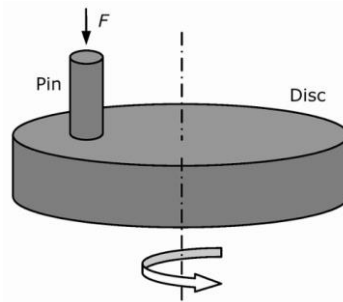


Figure 2.4: Pin-on-disk tribometer (Tribolab, 2008)

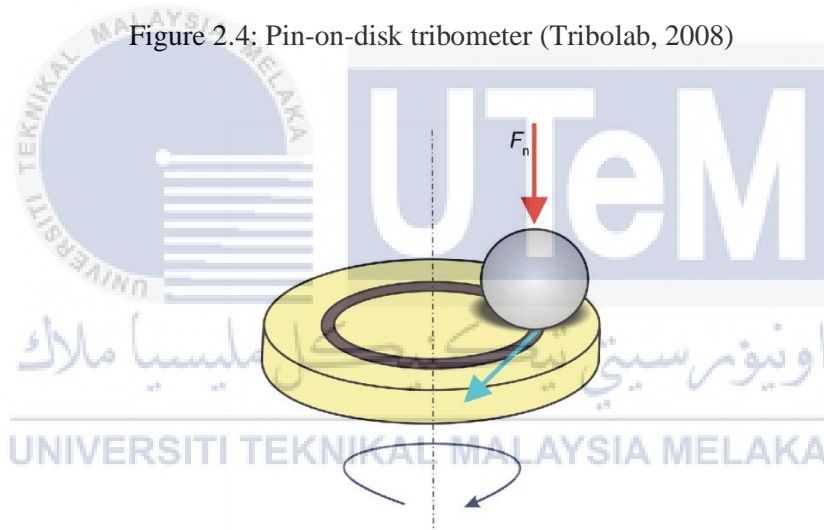


Figure 2.5: Ball-on-disk tribometer (Acta Metallurgica Sinica, 2014).

Elsheikh et al. (2020) and Verma et al. (2019) used pin-on-disk tribometer to perform experiment on their lubricants to determine the coefficient of friction and wear of their lubricants. All of them conducted the experiment based on ASTM G99. This is because by using ASTM G99 standard, they will have to conduct the test using same procedures, methods and parameters thus enable them to compare their result with the other studies that used the same ASTM G99 standard with ease. On the other hand, there were few authors conducted their test on lubricants with ball-on-disk tribometer (Hongmei et al., 2019; C. Li et al., 2019; Salah et al., 2017a; Wu et al., 2017; Xie et al., 2016). However, there is no ASTM standard mentioned in all 5 studies but one thing that is same for all of them. They

used AISI 52100 bearing steel ball for the contact body. By doing this, the inequality of the test can be reduced and so the comparison between different studies is possible.

Four Ball Tester is a test ran to determine the friction behaviour and wear properties of lubricants. It has the configuration of three steel balls at the bottom with one steel ball at the top. The top ball will be rotating ball which presses on the three bottom stationary balls while being immersed in the lubricants during the test as shown in Figure 2.6. The standard used for this test is ASTM D 2596 (extreme pressure), ASTM D 2266 (grease) and ASTM D 4172 (oils). The test will be conducted under a specified load, sliding speed, temperature and duration according to respective standard. Abdollah et al. (2020); Gao et al. (2019); Guzman et al. (2018); Ren et al. (2020); Talib et al. (2017) conducted their studies using ASTM 4172 Four Ball Tester. Table 2.6 shows the parameters used by the 5 studies and the parameters they used are similar because the standard they used was the same which is ASTM D 4172.

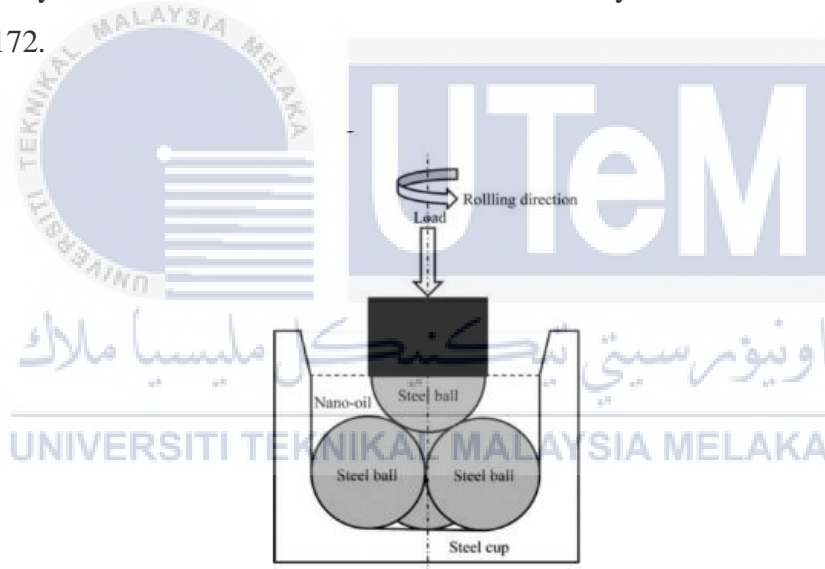


Figure 2.6: Diagram of Four Ball Tester (Abdullah et al., 2016).

Table 2.6: Parameters of Four Ball Tester used by the 5 studies.

References	Base oil	Additives	Load, N	Sliding Speed, rpm	Temperature, °C	Duration, min
Talib et al. (2017)	Modified jatropa oil	Hexagonal Boron Nitride	392	1200	75	60
Guzman et al. (2018)	Mineral oil, synthetic oil	Copper nanoparticles	392	1200	75	60
Abdollah et al. (2020)	Palm oil	Hexagonal Boron Nitride	392	1200	75	60
Ren et al. (2020)	Ester	Graphene	392	1200	40-100	60
Gao et al. (2019)	150N, PAO 4	Cholesterol ester liquid crystal	196	1200	75	30



Rheology is the study of the flow of matter namely solids, liquids and gases. According to Moreno (2001) and Struble and Ji (2001), rheology is explained as the review of flow behaviour and the science of deformation. It is usually applied to liquid materials that display time-dependent deformation over stress. O'Hara et al. (2014) stated that rheology is used as a technique to determine the viscosity on the effect of particle size of starting powder. The equipment that are usually used to run viscosity test are Redwood Viscometer and Capillary Viscometer.

### **2.3.1 Coefficient of friction**

Coefficient of friction is the ratio between friction force and normal force (Zhang, 2016). It does not have unit and is dimensionless. Not only that, the coefficient of friction value is different according to type of materials used (Behera and Hari, 2010). According to Ebnesajjad and Khaladkar (2005), coefficient of friction is directly proportional to velocity but inversely proportional to pressure. Furthermore, Behera and Hari (2010) announced that coefficient of friction are divided into two types which are coefficient of static friction and coefficient of kinetic friction. Coefficient of static friction is the ratio of static frictional force when two surfaces came in contact before motion acts to the normal force. On the other hand, coefficient of static friction is the ratio of kinetic frictional force when two surfaces came in contact during the motion to the normal force. Table 2.7 shows the coefficient of friction of some common base lubricants with additives. In the research done by Salah et al. (2019), as the concentration of CNTs increases, the coefficient of friction decreases. The coefficient of friction is at lowest value when the concentration is at 0.1 vol%. CNTs from carbon rich fly ash has active radical sites on the side wall where it assisted the adhesion of CNTs to the metal surface to reduce the friction. After 0.1 vol% concentration, the coefficient of friction starts to increase. This is because at higher concentration, the CNTs will form large clusters and these clusters may permeate within the oil due to the overlapping each other. Furthermore, the increase in coefficient of friction is because of the decrease in the stability of CNTs between two sliding surfaces during motion (Salah et al., 2019). The same pattern is also found in the research done by the same author but with different base oil whereby the coefficient of friction value decreases until CNTs is at 0.1 vol% concentrations and then increases drastically (Salah et al., 2017a). The results for hexagonal boron nitride with palm oil showed that 0.1 vol % has the lowest coefficient of friction value

(Abdollah et al., 2020). This is because by adding hexagonal boron nitride, a thin lubricating film is produced which helped in altering the type of friction from sliding to rolling. Abdollah et al. (2020) mentioned that hexagonal boron nitrides slide smoothly over each other because they adjusted themselves in a similar direction as the motion of the solid bodies. However, as the concentration of hexagonal boron nitride increases, the coefficient of friction also increases. The increased in coefficient of friction was caused by the agglomeration of the hexagonal boron nitride which led to increasing in shear strength. Khan et al. (2019) stated the reason that coefficient of friction value is reduced after additives are being introduced which is because of the mending effect of the additives. The additives form a protective film between lubricants and surfaces which get rid of direct contact and lowers shear strength of the additives. In the research by Liu et al. (2020), the reduction in coefficient of friction value when adding copper nanoparticles is due to the deposition of copper nanoparticles on the surface of the sliding steel which then form a deposition film. The reason is because copper nanoparticles are small in size, exhibit good ductility and can fill up the grooves of the steel surface. The pattern for Suresha et al. (2020) on the coefficient of friction value of graphene nanoplatelets with neem oil is different than the other researches. The coefficient of friction value decreases as the concentration increases. This is explained by Suresha et al. (2020) that the increasing of concentration of graphene nanoplatelets will increase the viscosity of the oil which will help in the formation of film to reduce the coefficient of friction further.

Table 2.7: Coefficient of friction of additives mixed with base oils at different concentrations.

Additives	Base oil	Concentration, %	Coefficient of friction	References
CNTs from carbon rich fly ash	150SN	0.025	0.145	Salah et al. (2019)
		0.05	0.133	
		0.1	0.120	
		0.2	0.132	
		0.3	0.149	
CNTs from carbon rich fly ash	Sunflower oil	0.005	0.119	Salah et al. (2017a)
		0.01	0.102	
		0.02	0.096	
		0.05	0.090	
		0.1	0.086	
		0.2	0.089	
		0.3	0.094	
CNTs from oil fly ash	100SN	0.1	0.119	Salah et al. (2017b)
	500SN		0.129	
	150BS		0.125	
Fly ash Modified fly ash Treated fly ash	Poly-alpha-olefin	0.2	0.095	Cao and Xia (2017)
			0.091	
			0.099	

Modified treated fly ash			0.093	
Hexagonal boron nitride	MJO1	0.05	0.033	Talib et al. (2017)
		0.1	0.034	
		0.5	0.034	
	MJO3	0.05	0.028	
		0.1	0.031	
		0.5	0.034	
	MJO5	0.05	0.022	
		0.1	0.025	
		0.5	0.029	
Hexagonal boron nitride	Palm oil	0.1	0.075	Abdollah et al. (2020)
		0.2	0.095	
		0.3	0.097	
		0.4	0.096	
		0.5	0.110	
SiO <sub>2</sub>	Deionised water	1	0.026	Cui et al. (2020)
		3	0.016	
		5	0.019	
TiO <sub>2</sub>		1	0.050	
		3	0.052	
		5	0.110	
ZnO		1	0.061	
		3	0.074	
		5	0.084	
SiO <sub>2</sub> : Graphene	Water	0.1: 0.4	0.066	Xie et al. (2019)
		0.2: 0.3	0.071	
		0.3: 0.2	0.144	
		0.4: 0.1	0.151	
SiO <sub>2</sub>	Sunflower oil	0.25	0.0141	Cortes et al. (2020)
		0.5	0.0154	
		0.75	0.0190	
TiO <sub>2</sub>		1	0.0124	
		1.25	0.0114	
		0.25	0.0111	
		0.5	0.0071	
		0.75	0.0032	
		1	0.0032	
MoS <sub>2</sub>	EOT5# engine oil	0.2	0.066	Xie et al. (2016)
		0.5	0.057	
		0.7	0.056	
SiO <sub>2</sub>		1	0.055	
		0.2	0.062	
		0.5	0.047	
		0.7	0.044	
Cu@SiO <sub>2</sub>	Distilled water	1	0.053	
		0.2	0.210	
		0.4	0.175	
SiO <sub>2</sub>		0.6	0.200	
		0.8	0.225	
		1.0	0.300	
		0.2	0.270	
		0.4	0.220	
		0.6	0.205	
		0.8	0.210	
		1.0	0.210	
TiO <sub>2</sub>	Deionised water	0.2	0.270	Wu et al. (2017)
		0.4	0.260	
		0.8	0.250	

		2.0	0.265	
		4.0	0.268	
		8.0	0.265	
Ni-MoS <sub>2</sub>	SN 500 mineral oil	0.1	0.0884	Rajendhran et al. (2018)
Bulk-MoS <sub>2</sub>		0.5	0.08	
		0.5	0.0885	
MoS <sub>2</sub>	Green cutting fluid (coconut oil, Azadirachta idica, Cymbopogon citratus, Centella asiatica, jaggery syrup)	0.3	0.307	Gajrani et al. (2019)
CaF <sub>2</sub>		0.3	0.315	
Graphene nanoplatelet	Neem oil	0.25	0.110	Suresha et al. (2020)
		0.5	0.088	
		0.75	0.084	
		1.0	0.070	
Cu	Virgin coconut oil	0.10	0.006	Khan et al. (2019)
		0.25	0.005	
		0.50	0.020	
		1.00	0.014	
Ag		0.10	0.007	
		0.25	0.009	
		0.50	0.027	
		1.00	0.017	
Graphene	Synthetic ester lubricant (SparkM40)	0.5	0.080	Ren et al. (2020)
		1.0	0.082	
		2.0	0.095	
Copper nanoparticles	Macadamia oil	0.1	0.078	Singh et al. (2019)
		0.2	0.075	
		0.3	0.070	
		0.4	0.086	
		0.5	0.092	
Copper nanoparticles	Paraffinic mineral	0.3	0.10	Guzman Borda et al. (2018)
		3.0	0.12	
	Synthetic ester	0.3	0.093	
		3.0	0.092	

### 2.3.2 Wear

Wear carries the meaning of removal of material or surface damage of material when in contact with an object in motion. Almost all cutting tools lose their durability and life span due to wear. Based on Straffelini (2015), wear rate changes dreadfully based on the operating conditions and material choices. According to Straffelini (2015), there are four main wear modes: Adhesive, abrasive, fatigue and corrosive wear. Adhesive wear is when fracture happened due to strong adhesion caused by plastic contact between two similar materials. Abrasive wear happens when fracture is produced during plastic contact between sharply hard material and soft material. This will form grooves and hollow on one of the materials.

Fatigue wear is generated when surface failed during repeated friction cycles of two contacts. Lastly, corrosive wear will be formed when there is a material removal phenomenon caused by tribochemical reaction. Table 2.8 shows wear reduction on some base lubricants with additives. The research by Wu et al. (2017) showed the highest wear reduction which is at 97.8% reduction. This is because at 0.8% concentration, TiO<sub>2</sub> nanoparticles are distributed evenly indicating that the spherical nanoparticles can roll between the two contacting surfaces in the friction motion. This “rolling effect” gives a compelling reduction of coefficient of friction thus highly reduces wear area. A concentration of higher than 0.8% will cause the nanoparticles to agglomerate and concentration of lower than 0.8% will lead to insufficient nanoparticles act between the two surfaces and both will cause increase in wear rate. On the other hand, hexagonal boron nitride with average of 35x10<sup>3</sup> nm particles size at 0.05% concentration with modified jatropha oil produced lowest value in wear reduction which is at 24%. This is because according to Ye et al. (2016), large particles size will erode the film and roughen the surface which limits wear reduction while smaller particles have the potential to reduce wear.

Table 2.8: Wear reduction of base lubricants with additives

Additives	Base Oil	Particle Size	Concentration, %	Wear Reduction	References
Ni-MoS <sub>2</sub>	SN 500	2µm	0.5	40-50%	Rajendhran et al. (2018)
Hexagonal Boron Nitride	MJO5	20x10 <sup>3</sup> to 50x10 <sup>3</sup> nm	0.05	24%	Talib et al. (2017)
TiO <sub>2</sub>	Deionised water	20 nm	0.8	97.8%	Wu et al. (2017)
Graphene Nanoplatelets	Neem oil	50 nm	1.0	41.4%	Suresha et al. (2020)

### 2.3.3 Viscosity

Viscosity is a measure of the resistant of lubricants to the flow (Noria, 2012). The higher the viscosity, the thicker the liquid (Bochem, 2013). For example, water has a lower viscosity than engine oil. Kotia et al. (2018) mentioned that load carrying capacity and viscous friction is decided by viscosity. Also, it is known that temperature affects the viscosity, and this is important in the field of lubrication. According to Singh et al. (2019), having a high viscosity index is an added advantage to the lubricant. Viscosity index is a measure of the change of viscosity with change of temperature. It is unitless and is used to

determine the behaviour of lubricants. A high viscosity index means the viscosity does not affect much with a slight change in temperature. Figure 2.7 and 2.8 shows the effect of temperature on the viscosity of nano-GCFs with MoS<sub>2</sub> and CaF<sub>2</sub>. Both figures show similar trend which is the reduction of viscosity as temperature increases. This is because the intermolecular forces of the cutting fluids molecules are being reduced due to thermal energy which causes them to move away from each other (Gajrani et al., 2019). However, the viscosity CaF<sub>2</sub> based nano-GCFs from Figure 2.8 is lower than MoS<sub>2</sub> based nano-GCFs from Figure 2.7. This can be attributed to the smaller particle size of CaF<sub>2</sub> than MoS<sub>2</sub>. Another observation can be made which is after the concentration of both CaF<sub>2</sub> and MoS<sub>2</sub> based nano-GCFs exceeds 0.3%, the viscosity decreases. This is because at 0.3% concentration, viscosity reaches saturation point. Therefore, concentration above 0.3% will be considered as excess concentration and will result in improper dispersion and sedimentation of particles. Table 2.9 shows the viscosity of some base lubricants with additives. Based on the table, deduction can be made that the viscosity of lubricants increased as the concentration of additives increased. This is because, as the concentration increases, the particles agglomerate and create bigger particles size which reduces the movement of fluid layers on each other (Suresha et al., 2020). To understand better about the viscosity behaviour, viscosity enhancement percentage for concentration range between 0% to 0.5% additives was calculated. Interestingly, lubricant from Singh et al. (2019) has the lowest viscosity enhancement although the viscosity is the highest which is at 77cP. In the research done by Khan et al. (2019), Ag nanoparticles blended with coconut oil has higher viscosity enhancement than Cu nanoparticles blended with coconut oil. This is because small particles will agglomerate easier than coarse particles (Wang et al., 2015).

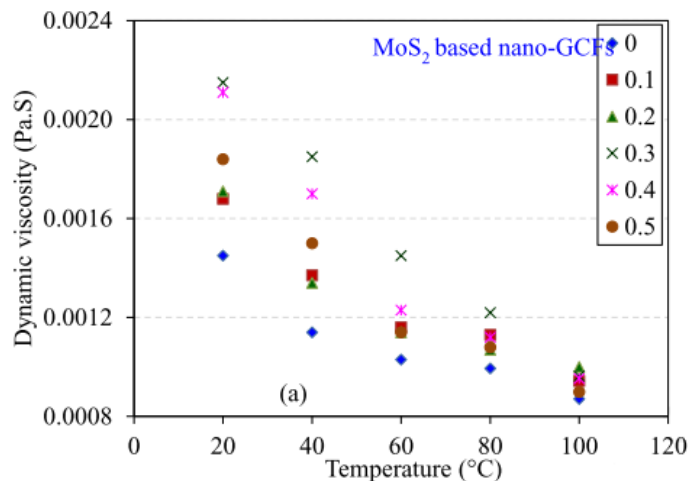


Figure 2.7: Dynamic viscosity of nano-green cutting fluid with MoS<sub>2</sub> (Gajrani et al., 2019).

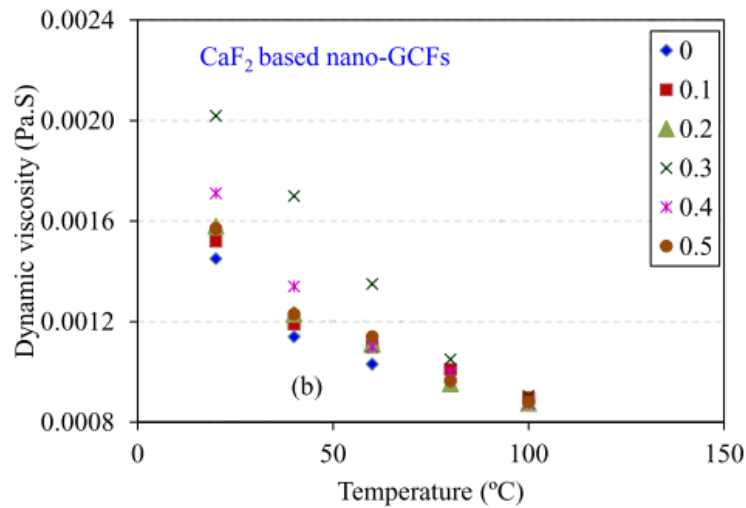


Figure 2.8: Dynamic viscosity of nano-green cutting fluid with CaF<sub>2</sub> (Gajrani et al., 2019).

Table 2.9: Viscosity of base lubricant with additives.

Additives	Base oil	Particle size	Concentration, %	Viscosity, cP	Viscosity enhancement, %	References
Graphene Nanoplatelets	Neem Oil	<50 nm	0	53.3	10.13	Suresha et al. (2020)
			0.25	55.5		
			0.5	58.7		
Cu Nanoparticles	Coconut oil	20-30 nm	0	30.0	70.00	Khan et al. (2019)
			0.1	49.9		
			0.25	50.0		
			0.5	51.0		
Ag Nanoparticles	10-20 nm	10-20 nm	0	30.0	96.67	
			0.1	57.9		
			0.25	58.0		
			0.5	59.0		
SiO <sub>2</sub>	Sunflower oil	20-30 nm	0	73	13.70	Cortes et al. (2020)
			0.25	81		
			0.50	83		
Cu Nanoparticles	Macadamia Oil	25 nm	0	77.0	2.73	Singh et al. (2019)
			0.1	77.5		
			0.2	78.0		
			0.3	78.4		
			0.4	78.7		
			0.5	79.1		

## 2.4 Surface Morphology

Surface morphology is a type of analytical imaging that produces images of samples that cannot be observed with naked eye by using complicated microscopes (Nanolab, 2018). It is a qualitative evaluation of the three-dimensional shape of a surface. In this study,

scanning electron microscope will be used to examine the surface morphology of the worn surface because according to Carter et al. (2015), scanning electron microscope is suitable for comprehensive study of a specimen's surface.

#### **2.4.1 Worn surface**

There are some studies that have done on worn surface analysis using different types of lubricants. In the study of Wang et al. (2018), they found that borate ester containing phenylboronic group mixed with PAO 6 base oil produced shallow furrows on the worn surface. This shows that the lubricant has a good tribological behaviour which able to avoid rubbing surfaces from direct contact with the steel ball from Four Ball Tester. Figure 2.9 shows the morphology of worn surface that were investigated by Cortes et al. (2020). According to the authors, the wear track, furrows and grooves formed are smooth and shallow due to the lubricant used was TiO<sub>2</sub> nanoparticles blended with sunflower oil. On the other hand, the lubricant containing SiO<sub>2</sub> nanoparticles has a rougher, harsher, deeper grooves and furrows than lubricant containing TiO<sub>2</sub> nanoparticles but both TiO<sub>2</sub> and SiO<sub>2</sub> nanoparticles gave smoother and shallower wear track than lubricant without nanoparticles. The change in morphology of the worn surface produced by TiO<sub>2</sub> and SiO<sub>2</sub> nanoparticles can be associated to the polishing effect which helped to reduce friction (Chang et al., 2005; Peng et al. 2010a). As for the different result between TiO<sub>2</sub> and SiO<sub>2</sub> nanoparticles on the worn surface, it is due to the size of the particles. Peng et al. (2010b) stated that lubricants with nanoparticles of larger size will increase the friction and thus causing rougher worn surface than smaller size nanoparticles. Therefore, when sunflower oil acts as base oil for lubricant, TiO<sub>2</sub> will give a smoother and shallower worn surface.



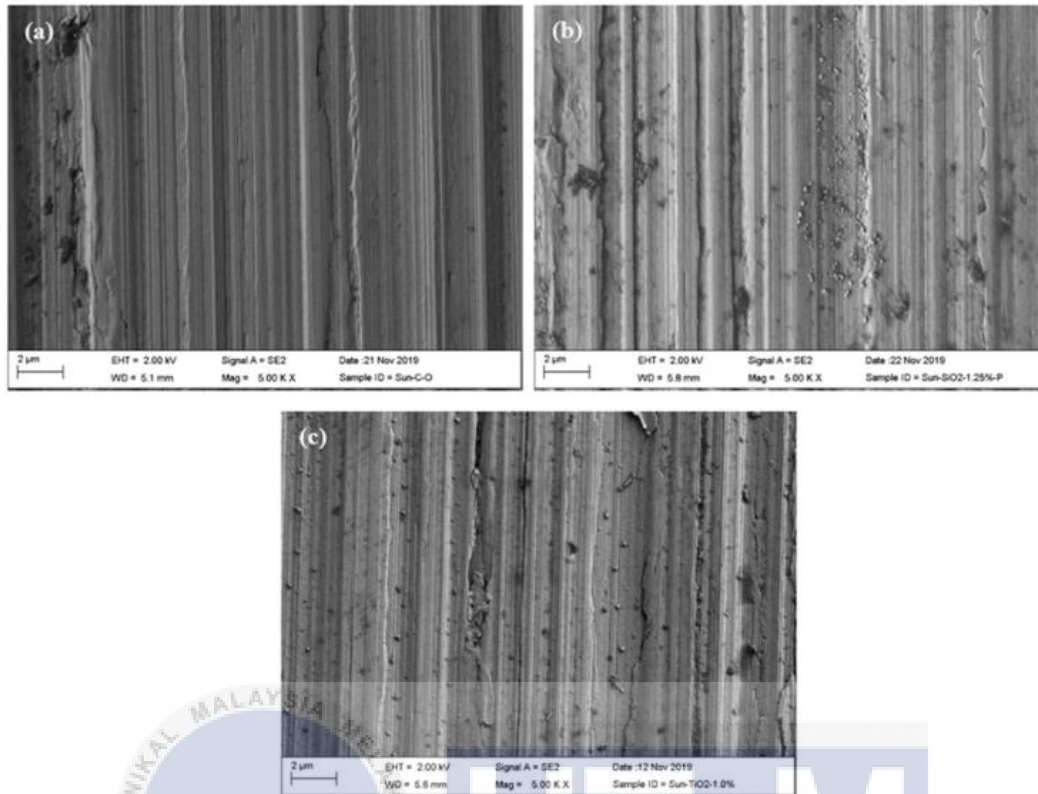


Figure 2.9: Morphology of worn surfaces produced during wear tests with (a) sunflower oil, (b) sunflower oil with SiO<sub>2</sub> nanoparticles at 1.25 wt.% and (c) sunflower oil with TiO<sub>2</sub> nanoparticles at 1.0 wt.% (Cortes et al., 2020).

#### 2.4.2 Surface roughness

According to Choudhury and Chinchankar (2017), surface roughness is defined as the measure of surface inconsistency which contained three parts: Roughness, waviness and form. Freyman et al. (2007) mentioned that tribological behaviour of surfaces is an important criterion of surface roughness. For example, of the important criterion is that deformation of surfaces can increase friction. Figure 2.10 shows surface roughness obtained by using different cutting fluids. Based on the Figure 2.10, canola oil produced the lowest surface roughness at 3.06 while mineral oil produced the highest surface roughness at 4.75. This is because canola oil has long carbon chain which able to form a coat between the workpiece and cutting tool thus reducing the heat produced (Shaikh and Boubekri, 2020). Furthermore, the author mentioned that the low value of surface roughness caused by canola oil is because canola oil has higher viscosity than mineral and synthetic oil. This helped reduce the frictional force between workpiece and cutting tool and abrasion of the cutting tool. Table

2.10 shows surface roughness obtained by other researches. The data shows similar pattern as the data in Figure 2.10 where bio-based oils produced lower surface roughness value than synthetic ester and polymeric lubricant. Therefore, deduction can be made that bio-based oil has better tribological behaviour than mineral and synthetic oils.

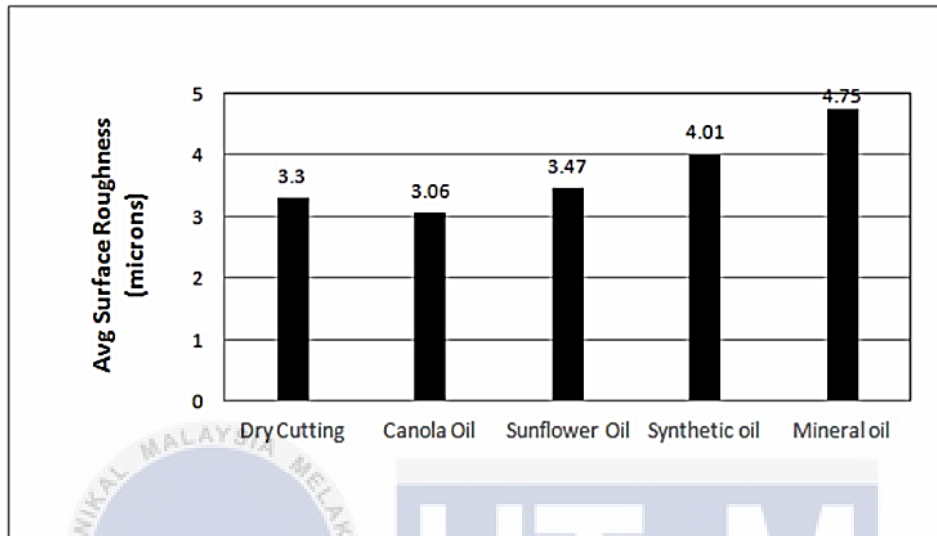


Figure 2.10: Surface roughness obtained by using different cutting fluid (Shaikh and Boubekri, 2020).

Table 2.10: Surface roughness obtained by other researchers.

Cutting Fluids	Surface Roughness (microns)	References
Canola Oil	0.232	Suresh et al. (2019)
Crude Jatropha Oil	0.13	Talib et al. (2017)
Modified Jatropha Oil	0.41	Talib et al. (2017)
Synthetic Ester	0.73	Talib et al. (2017)
Polymeric Lubricant	0.65	Peña-Parás et al. (2017)
Sunflower Oil	0.43	Cortes et al. (2020)
Macadamia Oil	0.15	Singh et al. (2019)

### 2.4.3 Wear scar diameter

Wear scar diameter is the measurement of diameter on the scar produced due to frictions between two objects and also defined as the lubricity of a fluid to act as a lubricant to reduce friction and damage to surface in contact under relative motion (Lam, 2017). The wear scar produced can be found on the surface of steel balls from the Four Ball Tester (Yadav et al., 2018). According to Yadav et al. (2018), wear scar diameter will increase when the temperature of lubricant increase. This is because increasing temperature causes

lubricant viscosity to be reduced thus creating only a thin film between two contacting surfaces. This thin film will eventually break down which will cause the wear scar diameter to increase. Figure 2.11 shows the wear scar diameter for 4 different concentration of biodiesel: B0 (Petrol-diesel), B2 (Petrol-diesel + 2% palm biodiesel), B5 (Petrol-diesel + 5% palm biodiesel) and B10 (Petrol diesel + 10% palm biodiesel). Based on the Figure 2.11, all 4 results showed increasing value in wear scar diameter as the temperature increased. A possible explanation given by Haseeb et al. (2010) is that increasing temperature decreases lubricant viscosity causing the boundary lubricant to breakdown thus bigger wear scar diameter will occurred. The decrease in wear scar diameter was due to the increment of viscosity of lubricant which helped in the formation of thin film (Suresha et al., 2020). Figure 2.12 shows the result of wear scar diameter at different concentration of GNPs-NO. From the figure, it is observed that pure neem oil showed darker grooves while GNPs at 1.0% concentration showed brighter grooves. Not only that, the wear scar diameter showed a decreasing trend. This is because the increment in concentration of GNPs increases the accumulations of GNPs at the concentric groove which then help in reducing the wear (Suresha et al., 2020).

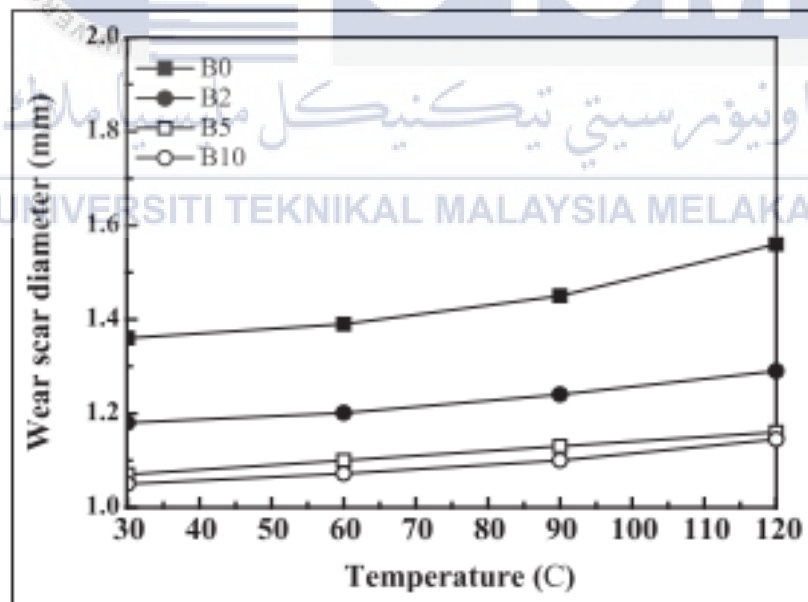


Figure 2.11: Wear scar diameter with temperature for different concentration of biodiesel (Peng, 2015).

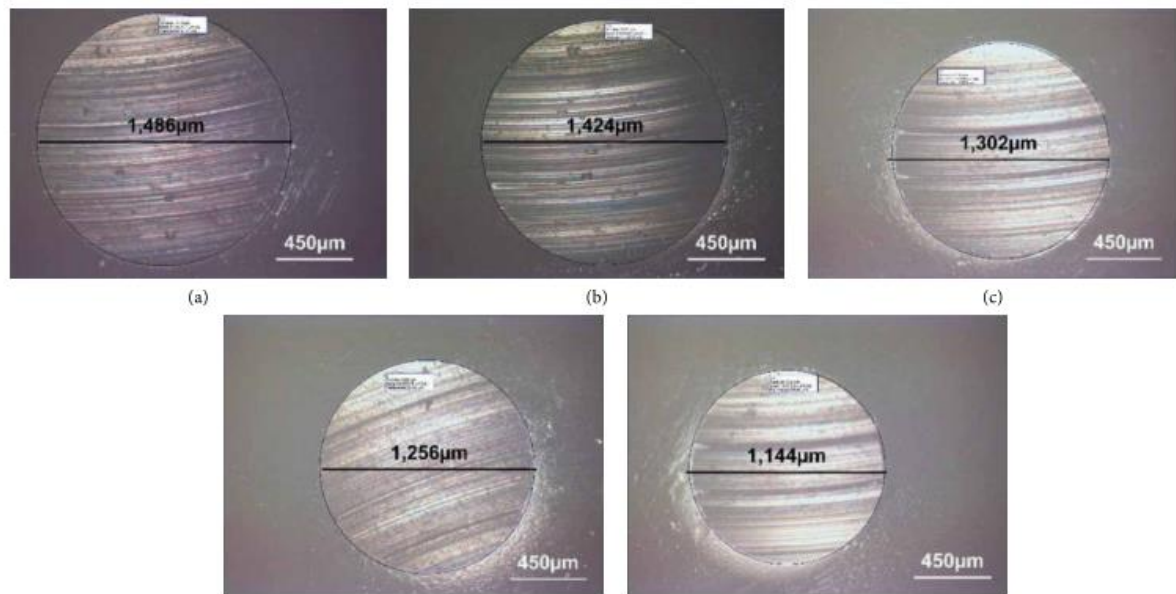


Figure 2.12: Optical micrograph of wear scar diameter: (a) pure neem oil, (b) 0.25% GNPs-NO, (c) 0.50% GNPs-NO, (d) 0.75% GNPs-NO and (e) 1.0% GNPs-NO (Suresha et al., 2020)

## 2.5 Additive Materials

Additives are elements that are used to improve the base oil performance as lubricants (Kopeliovich, 2012). They are usually mixed up with base oil with the range of 0.1% to 30% of base oil volume depending on the type of applications (Corporation, 2018). Other than enhancing performance of lubricants, additives are also able to contain unwanted properties or probably introduce new properties. According to Corporation (2018), additives are categorized into 3 types: Surface protective additives, performance additives and lubricant protective additives. Table 2.11 shows the general types of additives with their purpose, functions and example. The type of additives that are usually used to improve tribological behaviour of lubricants for machining processes are friction modifier and viscosity improver. This is because lubricant viscosity is one of the most important factor in affecting the tribological performance of the lubricant (Guo et al., 2020) and friction modifier is an additive to improve the lubricating ability of lubricant (Tang and Li, 2014). Tang and Li (2014) mentioned that the tribological behaviour of lubricants are depending on the particle size, composition, shape and concentration of additives in base oil. Figure 2.13 shows the wear scar diameter increases as the particle size increases. The reason is large particles size will act as abrasives and causing friction to increase during motion causing diameter of wear scar to increase (Peng et al., 2010b). According to Ermakov (2012),

additive composition is needed to enhance the properties of lubricant. For example, silicon dioxide particles in lubricant forms a protective nanocrystal-line film which assists in reducing friction (Ermakov, 2012). In term of additive shape, Jazaa and Chumbley (2018) believed that particles of spherical shape agreeable for rolling between contact surface and reducing friction. This is supported by Rawat et al. (2020) where spherical shaped nanoparticles showed good tribological behaviour as compared to other morphologies. Figure 2.14 shows the coefficient of friction value with different concentration of CNTs. From the figure, when the concentration of CNTs increases from 0 wt.% to 0.1 wt.%, the coefficient decreases However, higher concentration of additives in base oil does not always mean better. A directly proportional graph is shown on the figure at the 0.1 wt.% to 0.5 wt.% range. This is because an increment of concentration of additives leads to the agglomeration of particles which then forms bigger particles (Suresha et al., 2020). This will lead to an increase of shear strength thus increasing the coefficient of friction and wear scar diameter (Khan et al., 2019). A similar trend shown by Khan et al. (2019) in the study of copper and silver nanoparticles as additives in coconut oil. In their study, the concentration for both additives were set at 0.1%, 0.25%, 0.5% and 1%. After experiment was conducted using Pin-on-disk tribometer, it was found that copper nanoparticles at 0.25% and silver nanoparticles at 0.1% concentrations have shown the lowest coefficient of friction value. However, the coefficient of friction is at highest at 0.5% concentration for both additives. There are few research that have different trend as compared to the research by Khan et al. (2019) and Salah et al. (2017a). For example, research done by Suresha et al. (2020) showed a continuous downtrend for concentration of graphene nanoplatelets from 0.25 wt.% to 1.0 wt.%. The author stated that this reduction is associated to the increment in viscosity of lubricant. Not only that, no sign of coefficient of friction increasing is probably due to the concentration not high enough for the graphene nanoplatelets to agglomerate.

Table 2.11: General types of additives (Corporation, 2018)

<b>Surface Protective Additives</b>			
<b>Additive Type</b>	<b>Purpose</b>	<b>Typical Compounds</b>	<b>Functions</b>
<b>Anti-wear Agent</b>	Reduce friction and wear and prevent scoring and seizure	Zinc dithiophosphates, organic phosphates and acid phosphates; organic sulphur and chlorine compounds; sulphurized fats, sulphides and disulfides	Chemical reaction with the metal surface to form a film with lower shear strength than the metal, thereby preventing metal-to-metal contact
<b>Corrosion &amp; Rust Inhibitor</b>	Prevent corrosion and rusting of metal parts in	Zinc dithiophosphates, metal phenolates, basic	Preferential adsorption of polar constituent on metal surface to provide

	contact with the lubricant	metal sulfonates, fatty acids and amines	a protective film and/or neutralization of corrosive acids
<b>Detergent</b>	Keep surfaces free of deposits and neutralize corrosive acids	Metallo-organic compounds of barium, calcium and magnesium phenolates, phosphates and sulfonates	Chemical reaction with sludge and varnish precursors to neutralize them and keep them soluble
<b>Dispersant</b>	Keep insoluble soot dispersed in the lubricant	Polymeric alkylthiophosphates and alkylsuccinimides, organic complexes containing nitrogen compounds	Contaminants are bonded by polar attraction to dispersant molecules, prevented from agglomerating and kept in suspension due to solubility of dispersant
<b>Friction Modifier</b>	Alter coefficient of friction	Organic fatty acids and amines, lard oil, high molecular weight organic phosphorus and phosphoric acid esters	Preferential adsorption of surface-active materials
<b>Performance Additives</b>			
<b>Pour Point Depressant</b>	Enable lubricant to flow at low temperature	Alkylated naphthalene and phenolic polymers, polymethacrylates	Modify wax crystal formation to reduce interlocking
<b>Seal Swell Agent</b>	Swell elastomeric seals	Organic phosphates, aromatics, halogenated hydrocarbons	Chemical reaction with elastomer to cause slight
<b>Viscosity Improver</b>	Reduce the rate of viscosity change with temperature	Polymers and copolymers of methacrylates, butadiene olefins and alkylated styrenes	Polymers expand with increasing temperature to counteract oil thinning
<b>Lubricant Protective Additives</b>			
<b>Anti-Foaming</b>	Prevent lubricant from forming a persistent foam	Silicone polymers and organic copolymers	Surface tension reduced to speed collapse of foam
<b>Antioxidant</b>	Retard oxidative decomposition	Zinc dithiophosphates, hindered phenols, aromatic amines, sulphurized phenols	Decompose peroxides and terminate free-radical reactions
<b>Metal-Deactivator</b>	Reduce catalytic effect of metals on oxidation rate	Organic complexes containing nitrogen or sulphur, amines, sulphides and phosphites	Form inactive film on metal surfaces by complexing with metallic ions

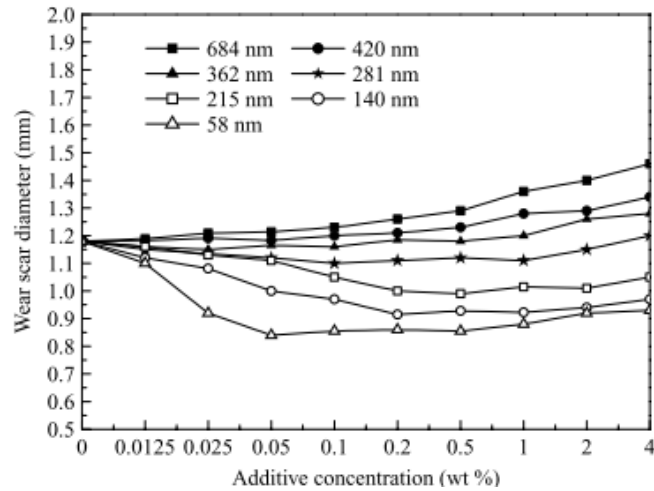


Figure 2.13: Wear scar diameter for variety of particle size (Peng et al., 2010).

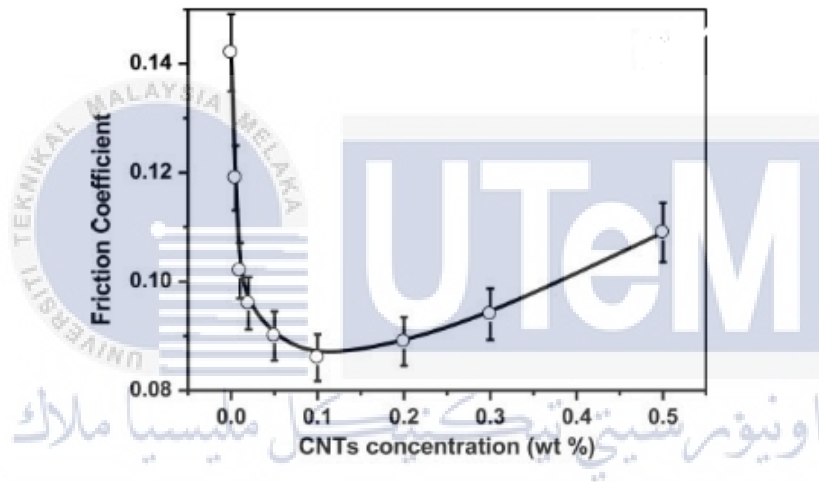


Figure 2.14: Friction coefficient against CNTs concentration (Salah et al., 2017a)

Researches were done to study on the tribological behaviour of different additives mixed with different base oils as lubricants. Table 2.12 shows the data for different additives mixed with different base oils together with the concentrations and coefficient of friction value. These data were collected from the recent 5 years of researches.

Table 2.12: Different types of additives mixed with different types of base oil.

Additives	Base oil	Concentration, %	References
CNTs from carbon rich fly ash	150SN	0.025, 0.1, 0.2, 0.3	Salah et al. (2019)
CNTs from carbon rich fly ash	Sunflower oil	0.005, 0.01, 0.02, 0.05, 0.1, 0.2, 0.3, 0.5	Salah et al. (2017a)
CNTs from oil fly ash	100SN 500SN 150BS	0.1	Salah et al. (2017b)
Fly ash Modified fly ash	Poly-alpha-olefin	0.2	Cao and Xia (2017)

Treated fly ash Modified treated fly ash			
Hexagonal boron nitride	MJO1 MJO3 MJO5	0.05, 0.1, 0.5 0.05, 0.1, 0.5 0.05, 0.1, 0.5	Talib et al. (2017)
Hexagonal boron nitride	Palm oil	0.1, 0.2, 0.3, 0.4, 0.5	Abdollah et al. (2020)
SiO <sub>2</sub> TiO <sub>2</sub> ZnO	Deionised water	1, 3, 5 1, 3, 5 1, 3, 5	Cui et al. (2020)
SiO <sub>2</sub> : Graphene	Water	0.1: 0.4 0.2: 0.3 0.3: 0.2 0.4: 0.1	Xie et al. (2019)
SiO <sub>2</sub> TiO <sub>2</sub>	Sunflower oil	0.25, 0.5, 0.75, 1, 1.25 0.25, 0.5, 0.75, 1, 1.25	Cortes et al. (2020)
MoS <sub>2</sub> SiO <sub>2</sub>	EOT5# engine oil	0.2, 0.5, 0.7, 1 0.2, 0.5, 0.7, 1	Xie et al. (2016)
Cu@SiO <sub>2</sub> SiO <sub>2</sub>	Distilled water	0.2, 0.4, 0.6, 0.8, 1.0 0.2, 0.4, 0.6, 0.8, 1.0	Liu et al. (2020)
TiO <sub>2</sub>	Deionised water	0.2, 0.4, 0.8, 2.0, 4.0, 8.0	Wu et al. (2017)
Ni-MoS <sub>2</sub> Bulk-MoS <sub>2</sub>	SN 500 mineral oil	0.1, 0.5 0.1, 0.5	Rajendhran et al. (2018)
MoS <sub>2</sub> CaF <sub>2</sub>	Green cutting fluid (coconut oil, Azadirachta idica, Cymbopogon citratu, Centella asiatica, jaggery syrup)	0.3 0.3	Gajrani et al. (2019)
Graphene nanoplatelet	Neem oil	0.25, 0.5, 0.75, 1.0	Suresha et al. (2020)
Cu Ag	Virgin coconut oil	0.1, 0.25, 0.5, 1.0 0.1, 0.25, 0.5, 1.0	Khan et al. (2019)
Graphene	Synthetic ester lubricant (SparkM40)	0.5, 1.0, 2.0	Ren et al. (2020)
Copper nanoparticles	Macadamia oil	0.1, 0.2, 0.3, 0.4, 0.5	Singh et al. (2019)
Copper nanoparticles	Paraffinic mineral Synthetic ester	0.3, 3.0 0.3, 3.0	Guzman Borda et al. (2018)



### 2.5.1 Fly ash

Fly ash is an ash produced from the burning of pulverized coal in a coal power generating plant and then carried into the air (Basham et al., 2007). It is usually in grey coloured powder form as shown in Figure 2.15. However, there are also different colour of fly ash depending on the chemical and mineral compositions (Rahman, 2018). Fly ash that contains lime will produce a lighter colour where unburned fly ash will have a dark to blackish colour (Rahman, 2018). Fly ash is a very fine material where the sizes of particles are in the range of 10 to 100 micron and the shape of fly ash is spherical glassy (Administration, 2017). According to Basham (2007), in the combustion chamber, mineral impurities rise to the hot exhaust gases. Then as the materials cool down, it solidifies and become fly ash which are then collected from the exhaust gases by bag house or electrostatic precipitators. According to Xing et al. (2019), unburned carbon content in fly ash caused the strength of fly ash to be reduced especially in concrete application. Hower et al. (2017) also stated that the inefficiency in combustion of coal were caused by the unburned carbon in fly ash and this prevented fly ash from being used in wide range of application. Therefore, there were methods introduced to separate unburned carbon from fly ash so that it will not become a huge waste of resources. The methods are sieving, gravity separation, electrostatic separation, froth flotation and oil agglomeration. Hower et al. (2017); Xing et al. (2019); Zhang et al. (2020) commended to use gravity separation method to separate unburned carbon from fly ash. This is because gravity separation method was able to produce qualified ash products with lower energy consumption, simpler method and environmentally friendly production when compare to other methods.



Figure 2.15: Fly ash (Rahman, 2018).

### 2.5.1.1 Elements of fly ash

Many studies were done to determine the chemical composition or elements of fly ash. Carette and Malhotra (1987) used inductively coupled argon plasma to determine the chemical composition of fly ash. 11 samples of fly ash where 6 from bituminous coal, 3 from subbituminous coal and 2 from lignite coal were evaluated. Figure 2.16 shows the chemical composition of all the fly ashes. From the figure, fly ash 1 to 6 show the highest silicon dioxide content at 40% of total weight. However, fly ash 3 and 4 seem unusual because they have higher iron content than silicon dioxide. Fly ash 5 and 6 have exceptionally high loss on ignition (LOI) content values at 9.72% and 6.89%. The fly ash from subbituminous coal have higher silicon dioxide content than the fly ash from bituminous coal and lignite coal. Furthermore, fly ash 7 to 11 have somewhat similar chemical compositions on calcium oxide content which is above 10%. They are called as high calcium fly ash because the calcium oxide content in the fly ashes is high.

Fly ash source	Type of coal*	Chemical composition† (% by weight)												
		SiO <sub>2</sub>	Al <sub>2</sub> O <sub>3</sub>	Fe <sub>2</sub> O <sub>3</sub>	CaO	MgO	Na <sub>2</sub> O	K <sub>2</sub> O	TiO <sub>2</sub>	P <sub>2</sub> O <sub>5</sub>	MnO	BaO	SO <sub>3</sub>	LOI‡
1	B	47.1	23.0	20.4	1.21	1.17	0.54	3.16	0.85	0.16	0.78	0.07	0.67	2.88
2	B	44.1	21.4	26.8	1.95	0.99	0.56	2.32	0.80	0.27	0.12	0.07	0.96	0.70
3	B	35.5	12.5	44.7	1.89	0.63	0.10	1.75	0.56	0.59	0.12	0.04	0.75	0.75
4	B	38.3	12.8	39.7	4.49	0.43	0.14	1.54	0.59	1.54	0.20	0.04	1.34	0.88
5	B	45.1	22.2	15.7	3.77	0.91	0.58	1.52	0.98	0.32	0.32	0.12	1.40	9.72
6	B	48.0	21.5	10.6	6.72	0.96	0.56	0.86	0.91	0.26	0.36	0.21	0.52	6.89
7	SB	55.7	20.4	4.61	10.7	1.53	4.65	1.00	0.43	0.41	0.50	0.75	0.38	0.44
8	SB	55.6	23.1	3.48	12.3	1.21	1.67	0.50	0.64	0.13	0.56	0.47	0.30	0.29
9	SB	62.1	21.4	2.99	11.0	1.76	0.30	0.72	0.65	0.10	0.69	0.33	0.16	0.70
10	L	46.3	22.1	3.10	13.3	3.11	7.30	0.78	0.78	0.44	0.13	1.18	0.80	0.65
11	L	44.5	21.1	3.38	12.9	3.10	6.25	0.80	0.94	0.66	0.17	1.22	7.81	0.82

\*B, bituminous; SB, subbituminous; L, lignite.

Figure 2.16: Chemical composition of fly ashes: Major and minor elements (Carette and Malhotra, 1987).

Another study was done recently by Kim et al. (2020) to determine the elements in fly ash. There were 20 samples taken from Class C fly ash and Class F fly ash with each having 10 samples. The chemical compositions of fly ashes were observed using automated scanning electron microscope (ASEM) and X-ray fluorescence (XRF). Figure 2.17 shows the chemical composition of all 20 samples of fly ashes and the result shows that the weight of element contents between ASEM and XRF are very close to each other. Class C fly ash is also known as subbituminous coal because of its high calcium oxide content in the fly ash at around 20%. While having a lower calcium oxide content, Class F fly ash has higher

silicon dioxide content than Class C fly ash. This is because Class F fly ashes came from the burning of bituminous coal. Class F fly ash F5 to F7 have a relatively high iron content than the other Class C fly ash and Class F fly ash. Furthermore, their loss on ignition content are also high which are at 2.4%, 1.8% and 2.2% respectively. From the two studies discussed, over 80% weight of fly ash are composed of major elements such as silicon dioxide (SiO<sub>2</sub>), aluminium oxide (Al<sub>2</sub>O<sub>3</sub>), calcium oxide (CaO) and iron (III) oxide (Fe<sub>2</sub>O<sub>3</sub>) while less than 20% weight of fly ash are minor elements like magnesium oxide (MgO), sulfur trioxide (SO<sub>3</sub>), sodium oxide (Na<sub>2</sub>O), potassium oxide (K<sub>2</sub>O), titanium dioxide (TiO<sub>2</sub>), phosphorus pentoxide (P<sub>2</sub>O<sub>5</sub>) and strontium oxide (SrO).

Fly ash		Chemical composition (% by mass)											LOI <sup>a</sup>
		SiO <sub>2</sub>	Al <sub>2</sub> O <sub>3</sub>	Fe <sub>2</sub> O <sub>3</sub>	CaO	MgO	SO <sub>3</sub>	Na <sub>2</sub> O	K <sub>2</sub> O	TiO <sub>2</sub>	P <sub>2</sub> O <sub>5</sub>	SrO	
C1	XRF	38.4	19.8	6.2	21.9	5.3	1.4	1.8	0.6	1.4	1.7	0.4	0.4
	ASEM	32.2	22.1	6.3	25.6	5.9	1.0	3.1	0.9	1.0	1.7	0.2	-
C2	XRF	36.2	19.9	6.7	24.0	5.2	1.4	1.7	0.5	1.4	1.4	0.4	0.2
	ASEM	35.8	19.2	5.6	26.9	5.5	1.0	3.0	0.9	0.7	1.2	0.2	-
C3	XRF	33.2	17.0	5.8	28.1	7.0	1.9	1.9	0.4	1.4	1.4	0.4	0.9
	ASEM	25.3	19.3	5.2	32.5	7.8	2.6	3.4	0.6	1.1	1.9	0.3	-
C4	XRF	37.6	23.2	5.5	21.8	4.2	1.0	1.7	0.6	1.6	1.6	0.4	0.2
	ASEM	29.9	24.5	5.3	26.2	4.9	1.4	3.0	0.8	1.4	1.7	0.9	-
C5	XRF	37.9	19.5	5.7	22.9	5.6	0.9	2.0	0.5	1.4	1.5	0.4	1.2
	ASEM	27.8	20.8	5.9	31.4	7.0	0.6	2.9	0.5	0.8	1.9	0.4	-
C6	XRF	37.0	20.6	5.3	15.6	3.6	2.9	9.2	0.7	1.3	0.7	0.7	0.7
	ASEM	35.1	23.3	3.0	15.0	4.0	2.0	13.4	0.6	1.1	1.6	0.9	-
C7	XRF	39.1	20.0	6.2	22.3	4.9	1.0	1.8	0.7	1.4	1.1	0.4	0.4
	ASEM	32.6	21.5	5.9	25.6	5.2	0.9	3.6	1.1	1.0	1.5	1.1	-
C8	XRF	40.0	20.9	5.9	21.5	5.0	0.8	1.6	0.7	-	-	-	0.2
	ASEM	40.1	22.6	4.5	19.4	5.7	0.8	3.7	0.9	0.6	1.4	0.1	-
C9	XRF	36.0	22.4	5.5	24.0	4.8	1.2	1.7	0.5	-	-	-	0.1
	ASEM	31.5	24.0	6.0	25.7	5.3	1.0	3.7	0.6	0.9	1.1	0.1	-
C10	XRF	35.9	18.0	6.7	25.8	6.1	1.8	1.8	0.4	1.2	0.8	0.5	0.2
	ASEM	36.0	19.3	5.1	22.7	7.8	2.0	4.7	0.6	1.0	0.3	0.5	-
F1	XRF	56.3	20.1	5.7	10.3	3.0	0.5	0.6	1.4	1.2	0.1	0.3	0.2
	ASEM	45.2	24.3	6.6	14.7	3.5	0.8	1.8	1.9	0.7	0.2	0.2	-
F2	XRF	52.0	16.4	4.4	18.7	2.9	0.9	0.8	0.9	1.0	0.3	0.2	1.2
	ASEM	50.4	20.9	3.9	17.1	3.7	0.5	1.0	1.4	0.7	0.1	0.3	-
F3	XRF	59.2	24.4	6.2	4.0	1.2	0.4	1.4	1.1	1.1	0.1	0.1	0.6
	ASEM	48.8	26.6	6.6	9.3	2.0	0.3	1.7	1.9	1.5	0.1	1.1	-
F4	XRF	49.7	24.2	4.7	12.9	3.3	0.7	1.0	0.6	1.7	0.5	0.3	0.2
	ASEM	45.3	27.4	4.0	14.6	3.6	0.7	1.5	0.6	1.1	0.4	0.8	-
F5	XRF	51.5	23.2	11.9	3.9	1.1	0.9	0.9	2.4	1.3	0.2	0.1	2.4
	ASEM	53.2	25.4	11.2	2.1	0.2	0.8	1.0	4.4	0.7	0.0	1.0	-
F6	XRF	49.0	20.9	16.1	4.9	0.9	1.6	1.1	2.5	1.1	0.1	0.0	1.8
	ASEM	51.8	25.7	12.3	2.5	0.3	0.7	1.6	4.1	0.7	0.1	0.2	-
F7	XRF	47.7	24.9	14.7	3.7	0.9	0.7	0.7	1.7	1.3	0.3	0.1	2.2
	ASEM	51.9	26.4	8.0	3.3	0.5	1.7	4.0	2.5	0.9	0.6	0.1	-
F8	XRF	56.9	22.6	4.6	7.3	2.3	0.3	1.7	1.2	-	-	-	0.5
	ASEM	56.9	23.9	3.4	6.2	2.1	0.1	4.1	1.7	0.3	1.2	0.1	-
F9	XRF	53.5	19.2	6.3	13.2	3.1	0.6	0.6	1.1	-	-	-	0.4
	ASEM	48.3	25.0	5.8	12.6	3.3	0.5	1.3	1.8	1.1	0.2	0.1	-
F10	XRF	57.7	24.5	4.1	8.1	2.0	0.3	0.2	0.9	-	-	-	0.5
	ASEM	53.6	27.8	2.8	10.5	2.5	0.5	0.3	1.3	0.4	0.3	0.0	-

<sup>a</sup>: Loss on ignition

Figure 2.17: Chemical composition of fly ashes: Class C fly ash and Class F fly ash (Kim et al., 2020).

### 2.5.1.2 Properties of fly ash

According to Bhatt et al. (2019), the physical properties of fly ash are fine and powdery particles with sphere shapes. It has the specific gravity of 1.6 to 3.1 and high specific area with low density. The colour of fly ash ranges between white to dark red, or brown depending on the amount of iron content and unburned carbon. Table 2.13 shows the physical properties of fly ash. Fly ash was graded into two grades: Grade I fly ash and Grade II fly ash. Grade I fly ash were acquired from bituminous coals while Grade II fly ash was acquired from lignite or subbituminous coals. There was a standard by ASTM C618 that categorized fly ash into two categories: Class C fly ash and Class F fly ash. Class C fly ash is the same as Grade II fly ash where it was produced from lignite or subbituminous coals and Class F fly ash was produced from bituminous coals. Fly ash has a chemical property where it increases the durability of concrete due to less air entrainment if the loss of ignition is low. According to Zhang et al. (2020) fly ash has good carbonation resistance in cement application because of its high filling property which can fill the empty spaces between particles and create voids between cement particles for better cement hydration. This hydration of cement will eventually lead to the formation of protective layer through reaction between calcium hydroxide and iron (II) oxide and iron (III) oxide which then prevent the steel bars in the concrete from corroding. Zhang et al. (2020) stated that fly ash can improve the water resistance of magnesium oxysulfate cement by reducing the volume deformation of the cement caused by the stress of expansion. Wang et al. (2020) mentioned that the filling property of fly ash helped in enhancing the compressive strength of concrete. Moreover, fly ash has variety of swelling potential depending on the value of plasticity index (PI). PI value of lower than 10 shows that the fly ash have a low swelling potential and PI value of higher than 20 shows a high swelling potential. Other than that, fly ash has low maximum dry density (MDD) but high optimum moisture content (OMC). This is because in the study of physical, chemical and geotechnical properties of coal fly ash, Bhatt et al. (2019) wrote that as the fly ash content increase in the mixture of soil-fly ash, the MDD decreased and OMC increased. Lastly, fly ash has wide range of permeability depending on the class and each permeability have its own applications. The permeability of fly ash is between  $10^{-4}$  to  $10^{-7}$  cm/sec.

Table 2.13: Physical properties of fly ash (Gamage et al., 2011).

Property	Maher and Balaguru (1993)	Mitash (2007)	Huang et al. (1995)	Muhardi (2010)
<b>Specific Gravity</b>	2.54	1.9-2.55	2.06	2.3
<b>Moisture Content</b>	13.60%		0.53%	19.75%
<b>Fineness</b>			13.80% in No. 325	0.6-0.001 mm
<b>LOI</b>			7.5	
<b>Maximum Dry Density</b>	1.65 g/cm <sup>3</sup>	0.9-1.6 g/cm <sup>3</sup>		1.53 g/cm <sup>3</sup> cc
<b>Uniformity coefficient</b>	2.5	3.1-10.7		
<b>Liquid Limit</b>	16.8			
<b>Permeability</b>	0.9 x 10 <sup>-5</sup> cm/s	10 <sup>-5</sup> -10 <sup>-3</sup> cm/s		4.87 x 10 <sup>-7</sup> cm/s
<b>Angle of Internal Friction</b>		30°-40°		23°-41°
<b>Cohesion</b>		Negligible		3-34 kPa
<b>Compression Index</b>		0.05-0.4		0.15
<b>Coefficient of Consolidation</b>				0.1-0.5 m <sup>2</sup> /year

### 2.5.1.3 Application of fly ash

Nath (2020) stated that fly ash is suitable for geopolymer reaction because of its high silica and alumina content. However, the reactivity of fly ash at standard temperature is relatively low which makes it difficult to utilize in bulk and this can be overcome by mixing with zinc slag. This is supported by Purbasari et al. (2020) where fly ash containing aluminosilicate oxide was able to produce geopolymer which can be used to remove heavy metal through adsorption method. Other than that, fly ash based geopolymer can be used to remove a cationic dye which was mentioned by Acisli et al. (2020). Also, Ramanathan et al. (2020) stated that aluminosilicates derived from fly ash can be used in medical applications such as bone engineering and in drug field. Modified fly ash was a good adsorbent due to its chemical and physical properties which was helpful in adsorbing heavy metals from wastewater (Huang et al., 2020). In the study done by Guo and Zhang (2020), fly ash was used as raw materials to produce autoclaved and modified wall blocks. Fly ash was also used for the production of green concrete which is an environmentally friendly concrete that has higher strength and durability than the common concrete as mentioned by Jiang et al. (2020); Millán-Corrales et al. (2020); Wang et al. (2020); Zhao et al. (2020). Based on Mobili et al. (2020), cements from calcium sulfoaluminate and alkali-activated fly ash were alternative binders to Portland cements where they exhibited low drying shrinkage and high water

permeability. Zhou et al. (2020) showed that fly ash can be used as filler for production of polymer material with low fire hazards. Nowadays, self-healing concrete is an aspect of sustainable structures because it has low maintenance cost and longer life span. Chindasiriphan et al. (2020) studied and found that increasing fly ash content in concrete mixture was able to promote self-healing ability of the concrete. On continuation of the sustainable topic, Li et al. (2020) realized that fly ash can be used as underground backfill materials which not only dispose of solid wastes, but also act as a surface subsidence control. Fly ash is also known for its ability to reduce swelling problems of soils. To support the statement, Blissett and Rowson (2012) said that the tendency for soils to absorb water can be reduced by adding fly ash to the soils and thus causing the swelling of the soil to be reduced. This is because by adding coal ash, the soil becomes grainier which holds lesser water. This can be used in applications such as driveways and pavements.

## 2.6 Parameters

Parameters are the numerical or measurable values that describe the systems. In the tribology test which will be conducted by Four Ball Tester, the important parameters are load, sliding speed and duration. Different parameters values will give different result. Therefore, to compare the result between other studies, standard is introduced. The standard that was used for this Four Ball Tester is ASTM D 4172. This standard will provide a set of parameters for the test which will produce results that can be compared to other studies results that used the same standard. For example, Abdollah et al. (2020) and Talib et al. (2017) conducted experiments on their lubricants using ASTM D 4172 Four Ball Tester. Therefore, they have the same parameters such as 392N load, 1200rpm sliding speed, 75°C temperature and 60 minutes duration. Table 2.14 shows the comparison between the two studies on the coefficient of friction of their lubricants with the same parameters and material concentrations. Based on the table, the comparison between two lubricants can be made easily due to the standard that they used. Through the table, conclusion can be made that crude jatropha oil provide lesser coefficient of friction than palm oil as base oil.

Table 2.14: Comparison between two lubricants on the coefficient of friction.

Additive *	Base oil	Additive concentration, %	Load, N	Sliding Speed, rpm	Temp, °C	Duration, min	COF*	References
------------	----------	---------------------------	---------	--------------------	----------	---------------	------	------------

hBN	Palm oil	0.1	392	1200	75	60	0.060	(Abdollah et al., 2020)
		0.2					0.055	
		0.3					0.060	
		0.4					0.070	
		0.5					0.070	
hBN	Crude Jatropha oil	0.05	392	1200	75	60	0.033	(Talib et al., 2017)
		0.1					0.034	
		0.5					0.034	

\*hBN, Hexagonal boron nitride; COF, Coefficient of friction



## **CHAPTER 3**

### **METHODOLOGY**

This chapter highlights the steps taken during this research study. There are primarily four parts which are the materials selection, preparation of bio-based lubricants, tribological test and surface morphology observation. Materials selection discussed on the reasons why the materials are used in this research and provides the details on material properties. Preparation of bio-based lubricant was described in detail on the steps conducted to prepare the materials prior to tribological test. Tribological test was used to determine the tribological behaviour of fly ash microparticles mixed with palm oil as lubricant at varying concentrations. Lastly, surface morphology observations analysed the worn surface produced on the steel balls using Four Ball Tester at different concentrations of fly ash microparticles. Figure 3.1 shows the flow chart of this research starting from materials selection until conclusion.



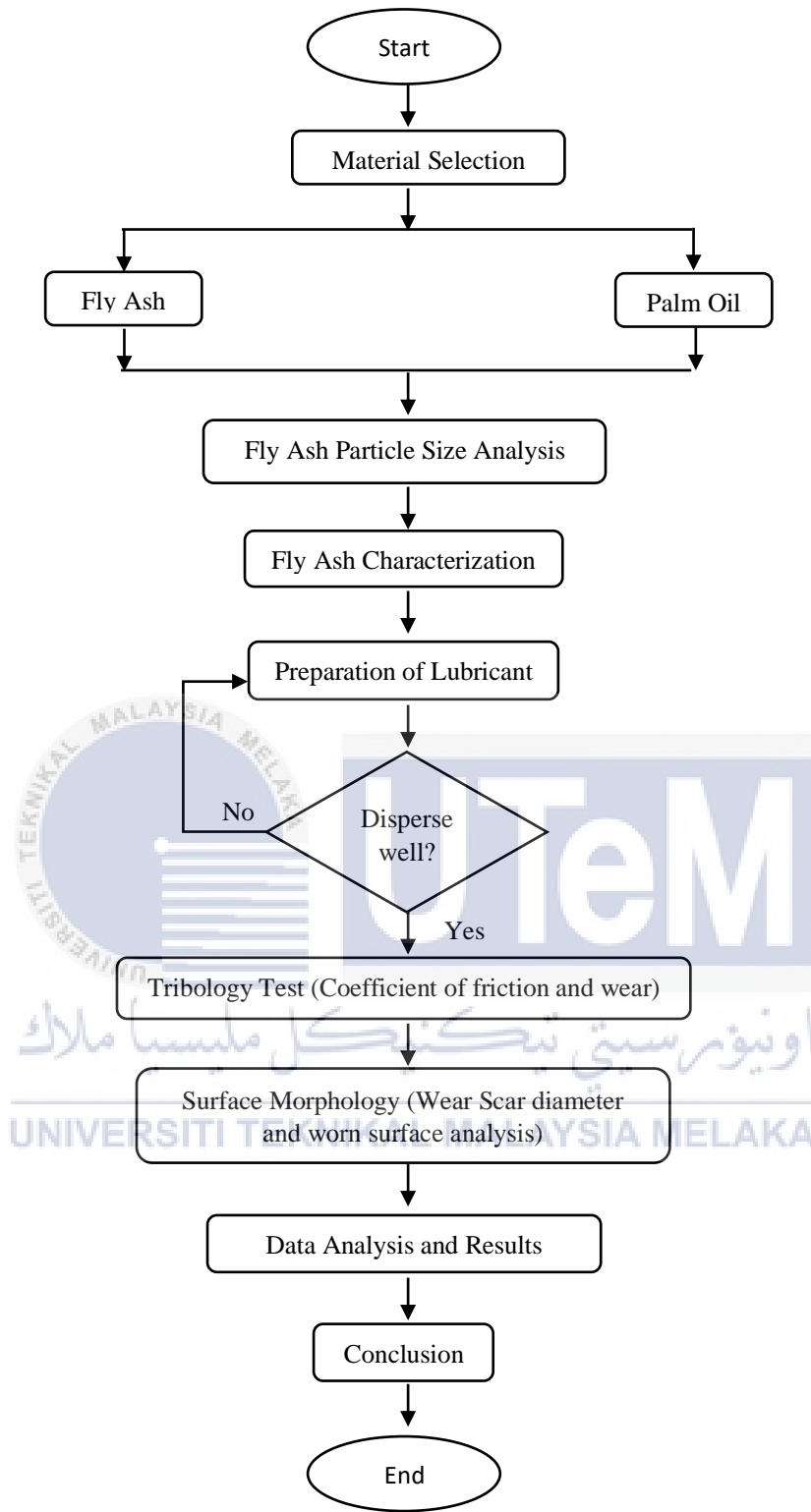


Figure 3.1: Research flow chart.

### 3.1 Materials Selection

#### 3.1.1 Characterization of fly ash

Fly ash microparticles from Department of Mineral and Geoscience Malaysia (JMG) under Ministry of Water, Land and Natural Resources was used. The size of fly ash microparticles was determined by using Malvern Mastersizer 2000 particle size analysis as shown in Figure 3.2. The size of fly ash microparticles was determined to be in the range between 0.50  $\mu\text{m}$  and 83.71 $\mu\text{m}$ . Chemical composition of the fly ash microparticles was characterized using PANalytical X'Pert Pro X-Ray Diffractometer as shown in Figure 3.3. Table 3.1 shows the chemical composition of the fly ash microparticles. Based on the table 3.1, fly ash microparticles contains 44.1% of  $\text{SiO}_2$ , 19.1% of  $\text{Al}_2\text{O}_3$ , 13.5% of  $\text{CaO}$ , and 12.4% of  $\text{Fe}_2\text{O}_3$ . According to ASTM C618-12 (2012), the fly ash microparticles is classified as Class F because the calcium oxide content in the fly ash microparticles is less than 20%. Figure 3.4 shows SEM image of fly ash microparticles (Intan et al., 2017).

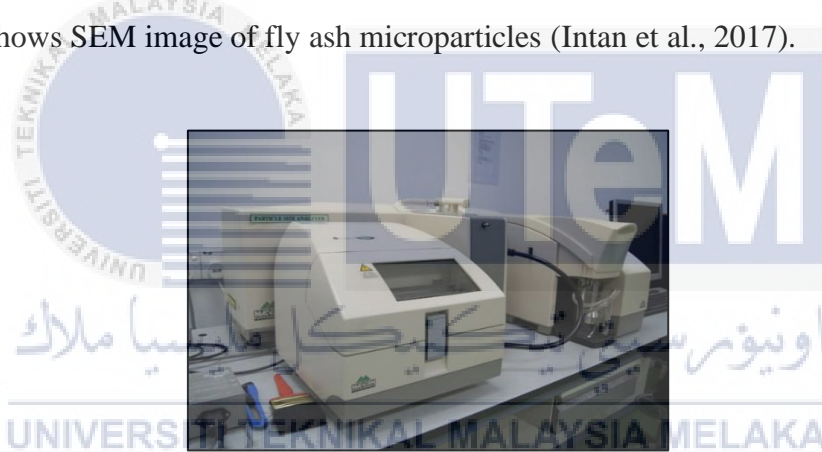


Figure 3.2: Particle size analysis (Malvern Mastersizer 2000).



Figure 3.3: X-Ray diffractometer (PANalytical X'Pert Pro)

Table 3.1: Chemical composition of fly ash microparticles.

Chemical Composition	Concentration (wt.%)
SiO <sub>2</sub>	44.1
Al <sub>2</sub> O <sub>3</sub>	19.1
CaO	13.5
Fe <sub>2</sub> O <sub>3</sub>	12.4
MgO	4.7
Na <sub>2</sub> O	2.9
K <sub>2</sub> O	1.4
SO <sub>3</sub>	1.0
TiO <sub>2</sub>	0.7
Mn <sub>2</sub> O <sub>3</sub>	0.1
P <sub>2</sub> O <sub>5</sub>	0.1

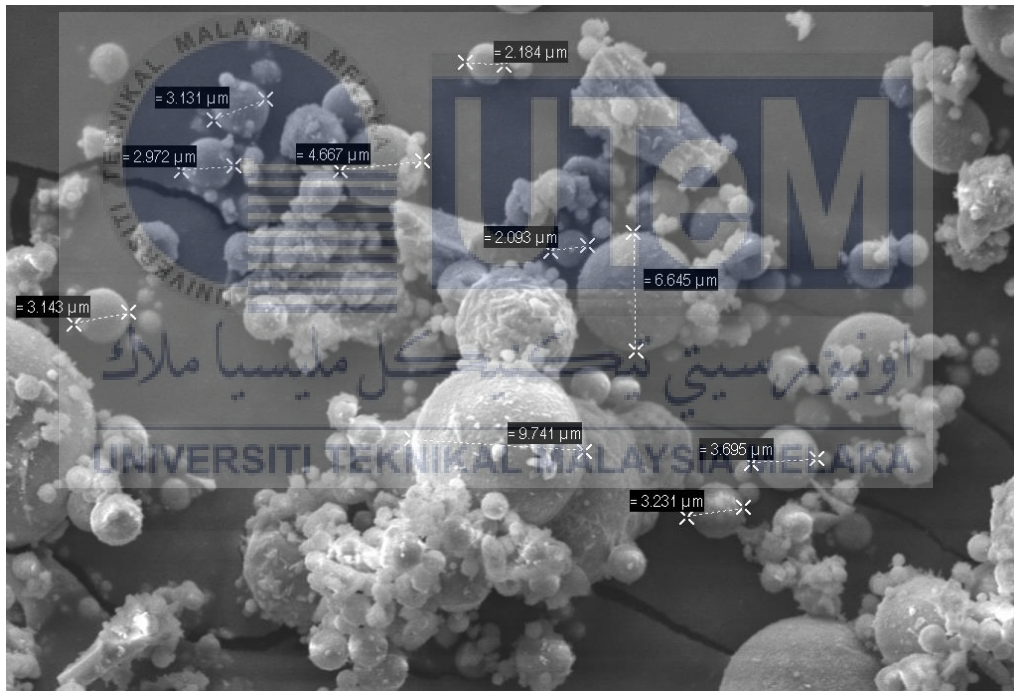


Figure 3.4: SEM image of fly ash microparticles (Intan et al., 2017).

### 3.1.2 Palm oil

Palm oil exists as reddish yellow liquid form with viscosity of 77cP at 25°C. The viscosity of palm oil increases drastically as the temperature increases by 5°C. Palm oil is not hazardous or chemically unstable as it is commonly used as cooking oil. It is widely

available especially in Malaysia because Malaysia palm oil contributes about 45.3% of palm oil productions in the world. Palm oil has a heat capacity of average 2kJ/kg°C and a density of 880kg/m<sup>3</sup>. Furthermore, palm oil has conductivity of higher than engine oil which is 0.17W/m°C. This shows that palm oil is also a good candidate to be used as base oil in lubricants. Table 3.2 shows the properties of palm oil.

Table 3.2: Properties of Malaysia palm oil (Department of Standards Malaysia, 2007).

Properties	Observed min. to max.
Apparent density, g/ml at 40°C	0.8969 – 0.8977
Refractive index, n <sub>0</sub> 40°C	1.4589 – 1.4592
Saponification value, mg KOH/g oil	194 – 202
Unsaponifiable matter, %	0.30 – 1.30
Fatty acid composition (wt % as methyl esters)	
C 12:0	0.2 – 0.4
C 14:0	0.9 – 1.2
C 16:0	38.2 – 42.9
C 16:1	0.1 – 0.3
C 18:0	3.7 – 4.8
C 18:1	39.8 – 43.9
C 18:2	10.4 – 12.7
C 18:3	0.1 – 0.6
C 20:0	0.2 – 0.6
Iodine value (Wijs)	56.0 – 59.1
Slip melting point, °	19.2 to 23.6
Total carotenoids (as β-carotene), mg/kg	500 to 1200
Colour at 40°C to 45°C	Bright, clear and deep red to reddish yellow
Odour	Free from foreign and rancid odour

### 3.2 Preparation of Bio-Based Lubricant

The preparation of the bio-based lubricant was conducted using ultrasonication process. The equipment used was an ultrasonic homogenizer from Faculty of Mechanical Engineering, Universiti Teknikal Malaysia Melaka. Figure 3.5 shows the ultrasonic homogenizer that was used for the ultrasonication process. A desired amount of fly ash (0.02 wt.%, 0.04 wt.%, 0.06 wt.%, 0.08 wt.%, 0.10 wt.%, 0.12 wt.% and 0.14 wt.%) was dispersed together with same ratio of Span 85 as surfactant into palm oil and then sonicated for 1 hour. The reason to use sonication rather than mechanical stirrer is to ensure fly ash is well dispersed in the palm oil. Then, the specimens were left for a day at room temperature to check for sedimentation. Table 3.3 shows the ratio to produce lubricants with different

concentration of fly ash microparticles in palm oil. The formula for the lubricant preparation is shown in Equation 3.1.

Table 3.3: Lubricants produced with different concentration of fly ash and palm oil.

Lubricant	Palm oil, g	Fly ash, g	Surfactant, g
Palm oil	100	0	0
Palm oil + 0.02 wt.% fly ash	100	0.01	0.01
Palm oil + 0.04 wt.% fly ash	100	0.02	0.02
Palm oil + 0.06 wt.% fly ash	100	0.03	0.03
Palm oil + 0.08 wt.% fly ash	100	0.04	0.04
Palm oil + 0.10 wt.% fly ash	100	0.05	0.05
Palm oil + 0.12 wt.% fly ash	100	0.06	0.06
Palm oil + 0.14 wt.% fly ash	100	0.07	0.07



Figure 3.5: Ultrasonic homogenizer

$$Wt\% = \frac{\text{Weight of solute (g)}}{\text{Weight of solution (g)}} \times 100\% \quad \text{Equation 3.1}$$

Where:

Weight of solute = Weight of Fly Ash + Weight of Surfactant

Weight of solution = Weight of Palm Oil

### 3.3 Tribological Test

Tribological tests on all the specimens were carried out in Tribology Laboratory at the Faculty of Mechanical Engineering, Universiti Teknikal Malaysia Melaka using Four Ball

Tribometer to determine the coefficient of friction of the lubricant. Figure 3.6 shows the Four Ball Tribometer that was used for the test. Figure 3.7 shows the schematic diagram of Four Ball Tribometer. The standard that was used on this study was the ASTM D 4172. Table 3.4 shows the ASTM standard and parameters that were used to conduct the tribology test. Four steel balls which are three named as stationary steel balls and one named as rotating steel ball were used. Before the test, all the steel balls were cleaned using acetone and then dried. The stationary steel balls were placed into the oil cup and then the coil cup was tightened using a torque wrench to prevent the stationary steel balls from moving during the test. The rotating steel ball was then tightened into the spindle of the machine. Next, the first specimen was introduced slowly to prevent air bubbles from forming. After that, the oil cup was installed into the disc securely. The next step was a test load of 392N was applied slowly onto the oil cup to prevent shock from happening. Then, the specimen was heated to a temperature of 75°C. After the set temperature was reached, the drive motor was set at speed 1200rpm to drive the spindle which holds the rotating steel ball. The test was conducted for a period of 1hour and after 1hour, the heater was turned off and oil cup was removed from the machine. Lastly, the specimen was drained from the oil cup and the scar area produced on the bottom three stationary steel balls was wiped and then sent to Scanning Electron Microscope for surface morphology observation. The test was performed thrice on the same concentration to ensure the reliability and accuracy of the results (Abdollah et al., 2020). The steps were repeated for different concentration of fly ash in palm oil. After the test, the coefficient of friction for each concentration was calculated using Equation 3.2. Then, the coefficient of friction for each concentration was averaged to achieve the result.

$$\text{Coefficient of friction, } \mu = \frac{T\sqrt{6}}{3Wr} \quad \text{Equation 3.2}$$

Where:

$T$  = Frictional force (Nm)

$W$  = Load

$r$  = distance from center of contact surface on lower balls to the axis of rotation = 3.67mm



Figure 3.6: Four ball tribometer.

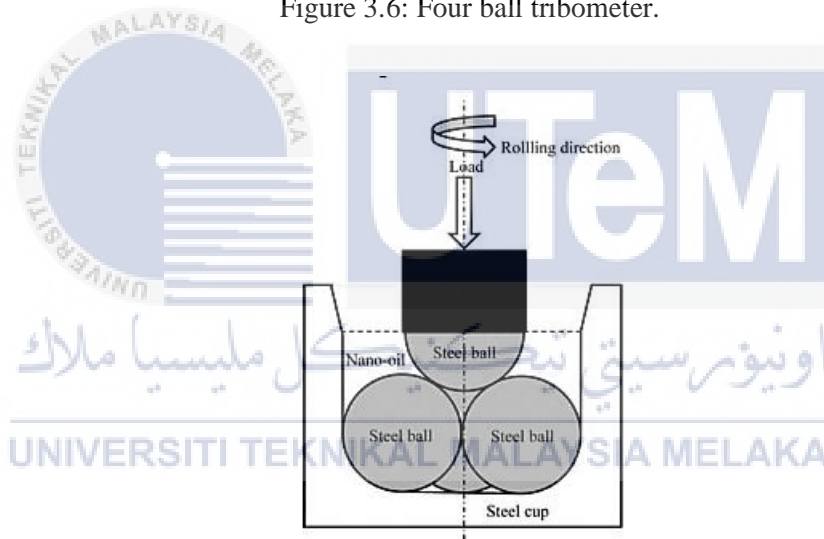


Figure 3.7: Schematic diagram of four ball tribometer.

Table 3.4: Parameter used to run Four Ball Tribometer.

Parameter	Load, N	Temperature, °C	Spindle rpm	Speed,	Duration, hr	Repetition, run
ASTM D 4172	392	75	1200		1	3

### 3.4 Surface Morphology Observation

Surface morphology observation was conducted on the steel balls for each concentration. The observations and analysis were carried out in the Tribology Laboratory and Material Science Laboratory at Faculty of Mechanical Engineering, Universiti Teknikal Malaysia Melaka by using 3D Non-contact Optical Profilometer and JEOL6010PLUS Scanning Electron Microscope as shown in Figure 3.8 and Figure 3.9 respectively. It was conducted after tribological tests were done. Surface morphology observation was first conducted once on each of the steel ball using 3D Non-contact Optical Profilometer to determine the wear scar diameter. Then, three best steel balls from each concentration were chosen to undergo Scanning Electron Microscopy. The worn surface and wear scar diameter of the steel balls were analysed and studied. The average wear scar diameter on the steel ball was calculated using Equation 3.3. Then, it was averaged again to achieve the result. Table 3.5 shows the experimental run for wear scar diameter.

$$\text{Average wear scar diameter, in } \mu\text{m} = \frac{HR_1 + VR_1 + HR_2 + VR_2 + HR_3 + VR_3}{6} \quad \text{Equation 3.3}$$

Where:

*HR* = Horizontal Reading of wear surface

*VR* = Vertical Reading of wear surface



Figure 3.8: Scanning Electron Microscopy (JEOL6010PLUS).





Figure 3.9: 3D Non-contact Optical Profilometer.

Table 3.5: Experimental run for wear scar diameter

Lubricant with Fly Ash Concentration, wt. %	Repetition, run	Steel Ball Horizontal Wear Reading			Steel Ball Vertical Wear Reading			Average Wear Scar Diameter for Each Run, $\mu\text{m}$	Average Wear Scar Diameter for 3 runs, $\mu\text{m}$
		1	2	3	1	2	3		
0	1								
	2								
	3								
0.02	1								
	2								
	3								
0.04	1								
	2								
	3								
0.06	1								
	2								
	3								
0.08	1								
	2								
	3								
0.10	1								
	2								
	3								
0.12	1								
	2								
	3								
0.14	1								
	2								
	3								

## CHAPTER 4

### RESULTS AND DISCUSSIONS

This chapter discussed the data collected after completing the sample preparation, tribological test and surface morphology observation. All the hypothesis and discussions will be stated and supported by the previous researches done by other researchers on the coefficient of friction, wear scar and wear scar diameter.

#### 4.1 Tribological Properties of Bio-Based Lubricants

##### 4.1.1 Coefficient of friction of steel ball on different fly ash microparticles concentrations

Table 4.1 and Figure 4.1 shows the coefficient of friction of steel ball on all concentrations of fly ash microparticles.

Table 4.1: Coefficient of friction.

Lubricants with Fly Ash Concentrations, wt. %	Coefficient of Friction			Average Coefficient of Friction	Percentage of reduction, %
	Run 1	Run 2	Run 3		
0.00	0.136	0.143	0.142	0.140	0
0.02	0.120	0.118	0.119	0.119	15
0.04	0.113	0.117	0.112	0.114	18.57
0.06	0.101	0.105	0.111	0.106	24.29
0.08	0.083	0.077	0.077	0.079	43.57
0.10	0.076	0.068	0.075	0.073	47.86
0.12	0.058	0.061	0.066	0.062	55.71
0.14	0.084	0.084	0.087	0.085	39.29

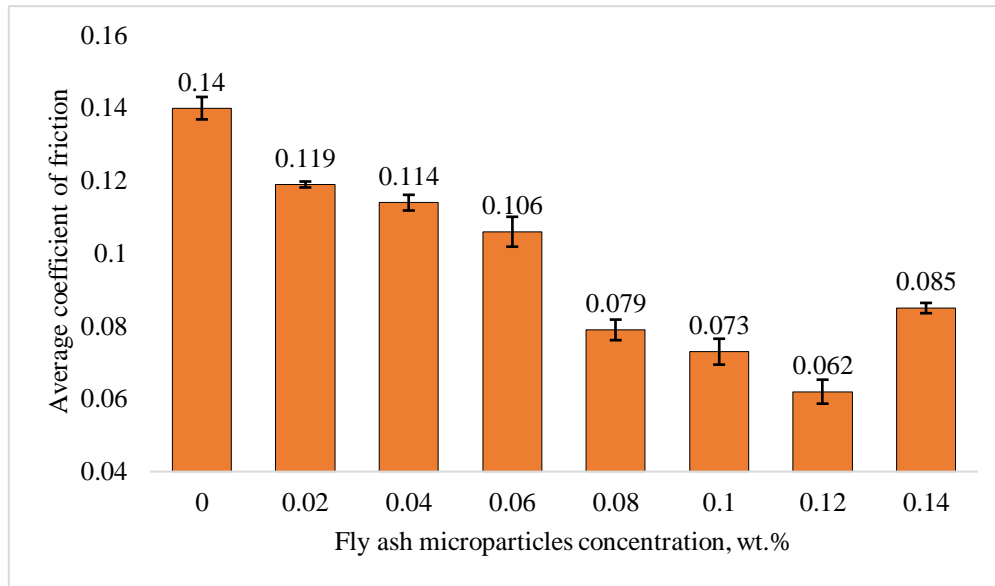


Figure 4.1: Coefficient of friction.

The coefficient of friction values for the bio-based lubricant samples ranged between 0.062 and 0.140. Based on the Figure 4.1, it was observed that pure palm oil (0.00 wt.%) has the coefficient of friction value of 0.14, which is the highest value among the eight bio-based lubricant samples tested. Evidently, with the addition of fly ash microparticles into palm oils, there were reductions in the coefficient of friction of the bio-based lubricant samples. As shown in Figure 4.1, 0.12 wt.% of fly ash microparticles possesses the lowest coefficient of friction, which is 55.71% lower than that of pure palm oil. The reason why there were reductions in coefficient of friction value after the addition of fly ash microparticles into palm oil was probably because of the ball-bearing effect caused by the fly ash microparticles. This effect changed the friction aspect from sliding to rolling. Figure 4.2 shows the schematic diagram of lubrication mechanism of microparticles.

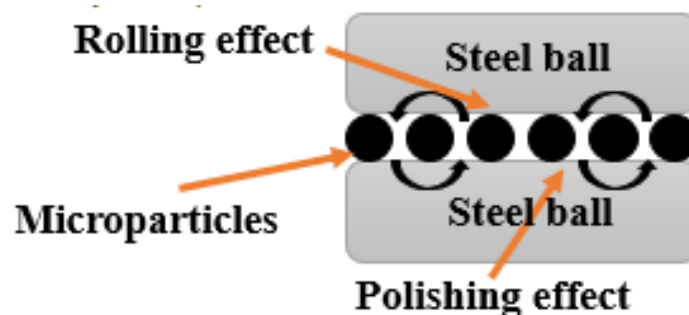


Figure 4.2: Schematic diagram of lubrication mechanism.

Based on the SEM image in Figure 3.4, the fly ash microparticles are having spherical shape and these spherical microparticles will flow in between the two contact surfaces thus causing the contacted surface to roll instead of sliding. This was in agreement with the findings of Xie et al. (2019) and Cortes et al. (2020).

However, when the fly ash concentration increased to 0.14 wt.%, the coefficient of friction increased instead of decreased. The increase in value of coefficient of friction at 0.14 wt.% of fly ash microparticles may be caused by the agglomeration of fly ash microparticles in the bio-based lubricants. According to Salah et al. (2017b) and Abdollah et al. (2020), agglomeration could formed at higher concentration of additives which led to a high coefficient of friction. Van der Waals forces could cause particles to clump together which will lead to agglomeration of particles during dispersion process (Werth et al., 2003). It is possible that at high fly ash microparticles concentration, the van der Waals forces are higher than dispersion forces, thus causing the microparticles to agglomerate and led to the increment of coefficient of friction.

#### 4.1.2 Wear scar diameter of steel ball

Table 4.2 and Figure 4.3 shows the wear scar diameter of steel balls after the wear test.

Table 4.2: Wear scar diameter.

Fly Ash Concentration, wt. %	Repetition, run	Steel Ball Horizontal Wear Reading			Steel Ball Vertical Wear Reading			Average Wear Scar Diameter for Each Run, $\mu\text{m}$	Average Wear Scar Diameter for 3 runs, $\mu\text{m}$
		1	2	3	1	2	3		
0	1	601.73	643.441	634.759	613.519	662.722	636.491	632.110	616.984
	2	634.202	589.014	611.138	609.738	601.388	610.066	609.258	
	3	645.077	593.182	606.38	597.865	598.741	616.267	609.586	
0.02	1	583.453	563.008	573.043	583.625	564.008	575.001	573.69	575.941
	2	589.074	566.607	575.591	588.366	570.131	572.618	577.065	
	3	592.15	578.64	597.713	586.984	535.008	571.911	577.068	
0.04	1	548.253	554.003	564.676	547.172	556.164	558.869	554.856	558.97
	2	605.013	536.015	603.083	574.008	534.004	562.001	569.021	
	3	544.697	553.024	555.643	549.239	569.88	545.723	553.034	
0.06	1	568.001	551.015	570.003	576.001	563.107	569.004	566.189	554.251
	2	530.917	551.832	576.63	532.819	552.85	564.929	551.663	
	3	550.206	547.168	547.269	554.22	528.092	542.45	544.901	
0.08	1	551.277	534.979	543.087	543.417	529.66	546.11	541.422	548.806
	2	571	547.045	556.014	568.001	564.001	566.008	562.012	
	3	540.949	552.431	537.073	540.529	543.872	543.054	542.985	
0.10	1	564.008	552.004	545.092	559.044	572.224	553.033	557.568	545.089
	2	522.563	567.435	538.283	530.321	574.442	502.627	539.279	
	3	541.076	532.36	545.38	536.671	531.36	543.678	538.421	
0.12	1	478.881	520.535	496.504	512.505	546.41	508.54	510.563	523.862
	2	522.911	501.85	535.285	524.303	507.977	534.748	521.179	
	3	554	510.063	554.001	555.001	514.004	552.004	539.846	
0.14	1	573.022	603.053	586.003	572.022	613.02	593.001	590.02	576.448
	2	590.775	552.274	544.294	593.273	565.39	579.2	570.868	
	3	557.593	585.618	565.838	562.377	569.14	570.165	568.455	

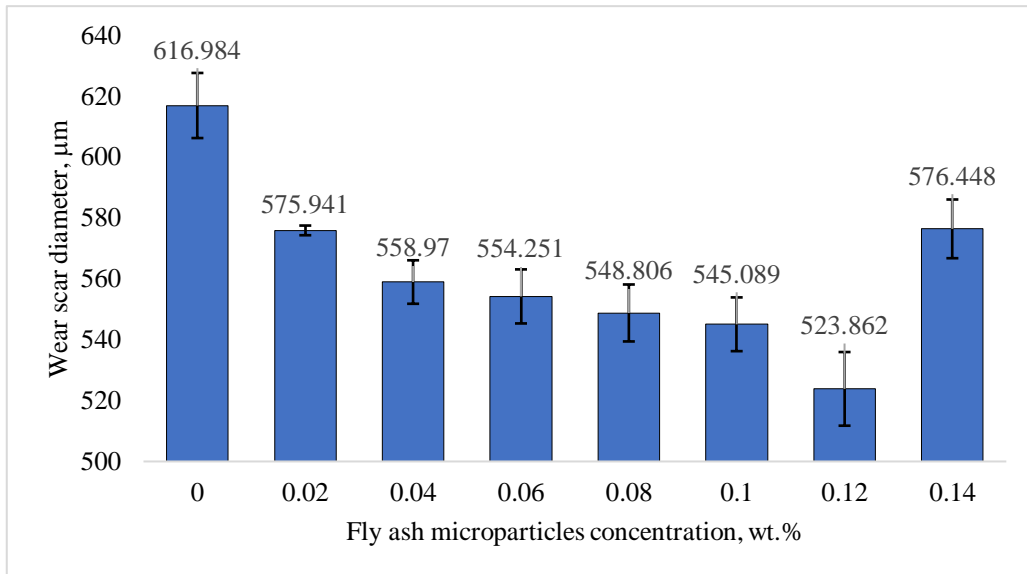


Figure 4.3: Wear scar diameter

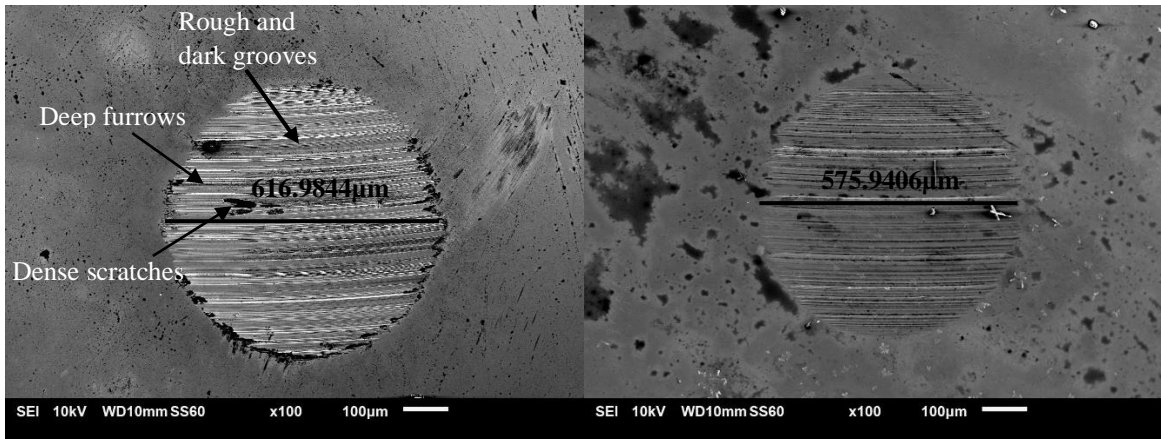
The wear scar diameter was calculated by using Equation 3.3. Based on Table 4.2, the average wear scar diameter for pure palm oil was the highest in comparison to palm oil filled with fly ash microparticles. This is because high coefficient of friction represents high deformation on steel ball surface, which is translated as high wear scar diameter. Then, as the concentration of fly ash microparticles in palm oil increases, the average wear scar diameter decreases until it reaches the optimum value at 0.12 wt.% of fly ash microparticles. When the concentration of fly ash increased further, the wear scar diameter also tends to increase. However, it is worth noting that the wear scar diameter that produced by 0.14wt.% fly ash is still lower compared to that of pure palm oil.

The addition of fly ash microparticles in pure palm oil significantly reduced the average wear scar diameter of steel ball. This is because microparticle additive has anti-wear mechanism that cause mixed lubrication or boundary lubrication to occur when the lubricant film between tribo-pairs becomes thinner (Asrul et al., 2013).

## 4.2 Surface Morphology Analysis of Steel Ball

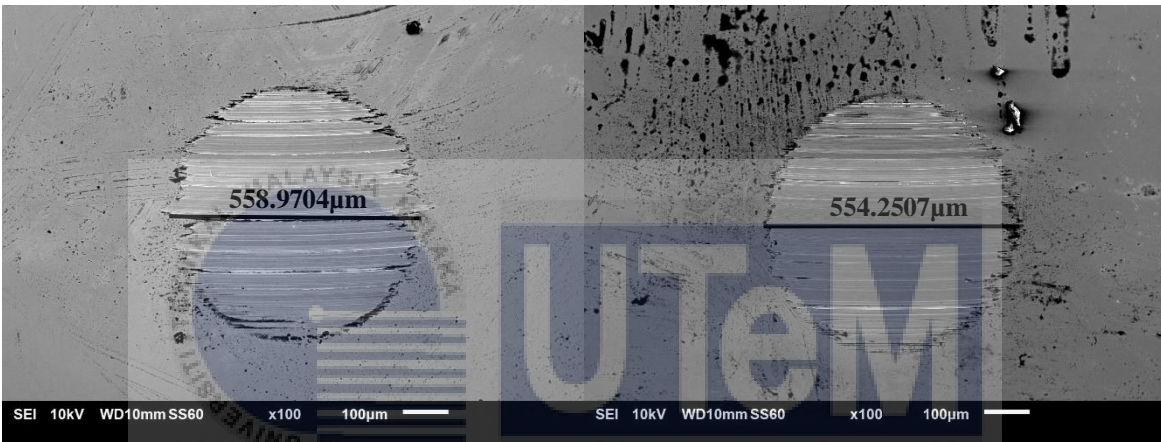
### 4.2.1 Observation by SEM

Figure 4.4 shows the SEM image of worn surface on steel balls for all the concentrations of fly ash microparticles.



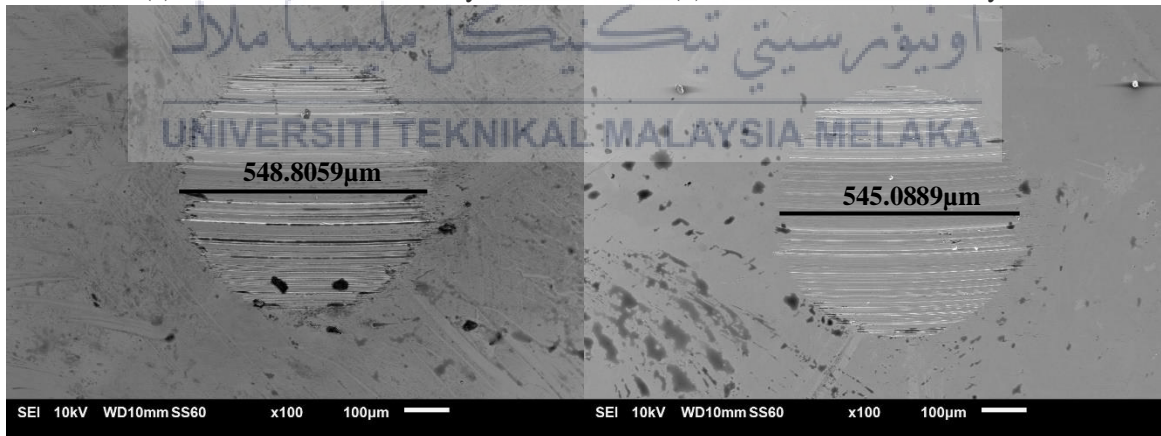
(a) Pure palm oil

(b) Palm oil + 0.02 wt.% fly ash



(c) Palm oil + 0.04 wt.% fly ash

(d) Palm oil + 0.06 wt.% fly ash



(e) Palm oil + 0.08 wt.% fly ash

(f) Palm oil + 0.10 wt.% fly ash

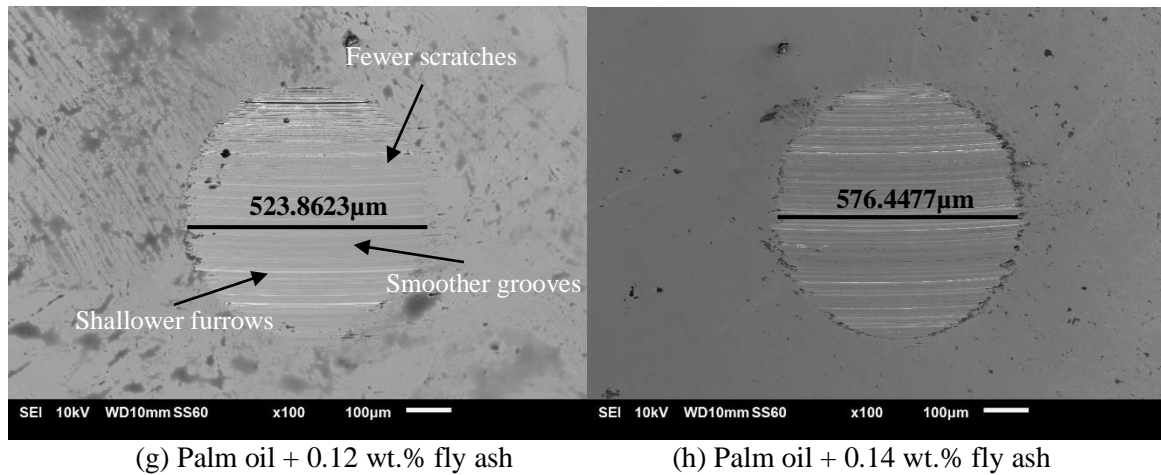


Figure 4.4: SEM image of worn surface on steel balls.

Based on the Figure 4.4(a), it was observed that by using pure palm oil, the steel ball shows harsh surface with various rough grooves, dense scratches and deep furrows. Not only that, darker grooves were found in Figure 4.4(a) too and it depicts the abrasive wear. As the concentration of fly ash microparticles in the palm oil increases, the worn surface shows brighter grooves and smoother wear track and these interpreting lesser surface contact between steel balls. By using 0.12 wt.% fly ash microparticles (Figure 4.4(g)), the steel ball shows the smoothest and brightest wear track with fewest grooves, scratches and shallow furrows. However, it is noticed that rougher grooves were observed in 0.14 wt.% fly ash microparticles. These results are consistent with the one reported in Section 4.1.1 and 4.1.2. The increment of coefficient of friction depicts that there is an abrasive wear which will cause wear scar diameter to increase and deeper furrows and rougher grooves on the worn surface. Singh et al. (2019), Peña-Parás et al. (2017) and Rawat et al. (2020) also found the similar patterns whereby after the optimum concentration of additives, coefficient of friction value increases and causes the wear scar diameter to increase.



## **CHAPTER 5**

### **CONCLUSIONS AND RECOMMENDATIONS**

This chapter concludes the significant findings from the research on tribological behaviour of palm oil mixed with fly ash microparticles as a bio-based lubricant.

#### **5.1 Conclusions**

This study is focused on the effect of different concentration of fly ash microparticles in palm oil on the coefficient of friction, wear scar diameter and worn surface of the steel ball. There were eight different concentrations of fly ash microparticles were used in the research, namely 0.00 wt.% (pure palm oil), 0.02 wt.%, 0.04 wt.%, 0.06 wt.%, 0.08 wt.%, 0.10 wt.%, 0.12 wt.% and 0.14 wt.%. The bio-based lubricants were prepared using palm oil as base oil, fly ash microparticles as lubricant additive and Span 85 as surfactant. The tribological behaviour of these eight concentrations were examined during the research. The significant findings of the study are summarized as follows:

- (a) Addition of fly ash microparticles in the palm oil gives a better tribological behaviour than pure palm oil.
- (b) The coefficient of friction, wear scar diameter and worn surface can be significantly reduced with the addition of fly ash microparticles.
- (c) The optimum concentration is at 0.12 wt.% where it reduced the coefficient of friction and wear scar diameter by 55.71% and 15.09%, respectively compared to that of pure palm oil.
- (d) With the addition of 0.12 wt.% of fly ash, the worn surface has the smoothest grooves and shallowest furrow.

## 5.2 Recommendations

After gone through this research, there are various recommendations suggested to improve this study in the future. Future studies on the current topic are recommended to:

- (a) Use other bio-based oil as the base oil while maintaining fly ash microparticles as the additives and investigate the rheological behaviour between the bio-based lubricants.
- (b) Use FESEM to further inspect the worn surfaces of steel ball to prove that there is agglomeration occurred in higher concentration of fly ash microparticles.
- (c) Conduct EDS analysis on the worn surfaces of steel ball to prove that SiO<sub>2</sub> particles were directly involved during the wear test.

## 5.3 Sustainability Element

From this study, the elements of sustainability have been identified as below:

- (a) In the bio-based lubricant, the addition of fly ash microparticles assist in decreasing the coefficient of friction thus reducing the wear scar diameter and smoothing the worn surface of the steel ball.
- (b) The use of palm oil in the bio-based lubricant will help to reduce the usage of mineral oil and synthetic oil lubricant application. This is because palm oil is a biodegradable material hence the disposal of the bio-based lubricant will pose lesser threat to the environment than mineral or synthetic oil.
- (c) The use of fly ash as additives in the bio-based lubricant will help to reduce the disposal of fly ash into the landfill which will lead to lesser environmental pollution.

## 5.4 Lifelong Learning and Basic Entrepreneurship Element

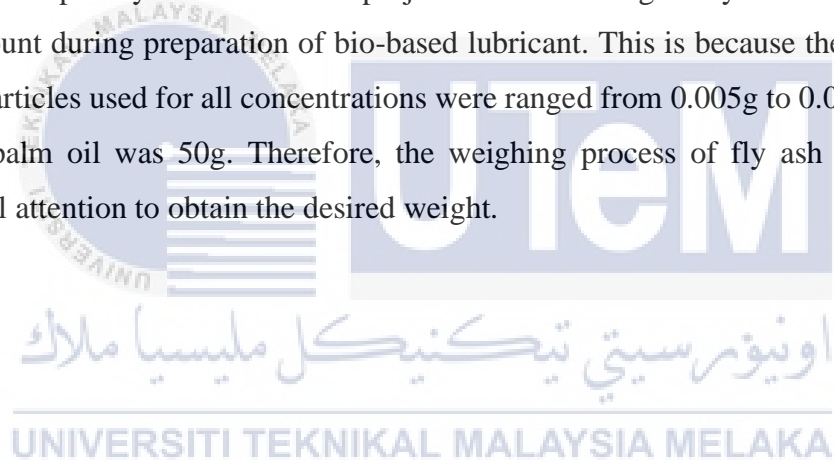
In this study, the lifelong learning is acquiring and expanding the knowledge. The knowledge obtained in the research which was the tribological behaviour of the bio-based

lubricant is gained and can be applied in the future research for improvement. Not only that, it provides extra knowledge and will be in great use to those who work in similar field.

There is potential to commercialize this bio-based lubricant because it is a biodegradable lubricant which gives less or no harm to the environment during disposal. Not only that, the cost of the materials is cheaper than the conventional lubricants and this will save the production cost of lubricant if it is to be commercialized. However, some researches were required to determine the method on mass producing this bio-based lubricant.

### **5.5 Complexity Element**

The complexity element in this project is the handling of fly ash microparticles in minute amount during preparation of bio-based lubricant. This is because the weight of fly ash microparticles used for all concentrations were ranged from 0.005g to 0.035g due to the weight of palm oil was 50g. Therefore, the weighing process of fly ash microparticles required full attention to obtain the desired weight.



## REFERENCES

- Abdollah, M. F. Bin, Amiruddin, H., & Jamallulil, A. D. (2020). Experimental analysis of tribological performance of palm oil blended with hexagonal boron nitride nanoparticles as an environment-friendly lubricant. *The International Journal of Advanced Manufacturing Technology*, 106(9–10), 4183–4191. <https://doi.org/10.1007/s00170-019-04906-5>
- Acisli, O., Acar, I., & Khataee, A. (2020). Preparation of a fly ash-based geopolymer for removal of a cationic dye: Isothermal, kinetic and thermodynamic studies. *Journal of Industrial and Engineering Chemistry*, 83, 53–63. <https://doi.org/10.1016/j.jiec.2019.11.012>
- Asrul, M., Zulkifli, N. W. M., Masjuki, H. H., & Kalam, M. A. (2013). Tribological properties and lubricant mechanism of nanoparticle in engine oil. *Procedia Engineering*, 68, 320–325. <https://doi.org/10.1016/j.proeng.2013.12.186>
- Bart, J. C. J., Gucciardi, E., & Cavallaro, S. (2013a). Biolubricant product groups and technological applications. *Biolubricants*, 565–711. <https://doi.org/10.1533/9780857096326.565>
- Bart, J. C. J., Gucciardi, E., & Cavallaro, S. (2013b). Lubricants: properties and characteristics. *Biolubricants*, 24–73. <https://doi.org/10.1533/9780857096326.24>
- BARTZ, W. J. (1974). Lubrication and Lubricants. *Vdi-Z*, 116(12 (AUGUST, 1974)), 1013–1021. [https://doi.org/10.1243/jile\\_proc\\_1921\\_011\\_030\\_02](https://doi.org/10.1243/jile_proc_1921_011_030_02)
- Behera, B. K., & Hari, P. K. (2010). Friction and other aspects of the surface behavior of woven fabrics. *Woven Textile Structure*, 230–242. <https://doi.org/10.1533/9781845697815.2.230>

- Bhatt, A., Priyadarshini, S., Acharath Mohanakrishnan, A., Abri, A., Sattler, M., & Techapaphawit, S. (2019). Physical, chemical, and geotechnical properties of coal fly ash: A global review. *Case Studies in Construction Materials*, *11*, e00263. <https://doi.org/10.1016/j.cscm.2019.e00263>
- Blissett, R. S., & Rowson, N. A. (2012). A review of the multi-component utilisation of coal fly ash. *Fuel*, *97*, 1–23. <https://doi.org/10.1016/j.fuel.2012.03.024>
- Campañá, C. E., & Müser, M. H. (2007). Theoretical studies of superlubricity. *Superlubricity*, 39–56. <https://doi.org/10.1016/B978-044452772-1/50034-2>
- Campanella, A., Rustoy, E., Baldessari, A., & Baltanás, M. A. (2010). Lubricants from chemically modified vegetable oils. *Bioresource Technology*, *101*(1), 245–254. <https://doi.org/10.1016/j.biortech.2009.08.035>
- Cao, Z., & Xia, Y. (2017). Study on the Preparation and Tribological Properties of Fly Ash as Lubricant Additive for Steel/Steel Pair. *Tribology Letters*, *65*(3), 104. <https://doi.org/10.1007/s11249-017-0885-x>
- Carette, G. G., & Malhotra, V. M. (1987). Characterization of Canadian fly ashes and their relative performance in concrete. *Canadian Journal of Civil Engineering*, *14*(5), 667–682. <https://doi.org/10.1139/187-097>
- Carter, M., Shieh, J., Carter, M., & Shieh, J. (2015). Chapter 5 – Microscopy. *Guide to Research Techniques in Neuroscience*, 117–144. <https://doi.org/10.1016/B978-0-12-800511-8.00005-8>
- Chan, C.-H., Sook Wah Tang, Noor Khairin Mohd, W. H. L., Yeong, S. K., & Idris, Z. (2018). Tribological behavior of biolubricant base stocks and additives. *Renewable and Sustainable Energy Reviews*, *93*, 145–157.
- Chang, L., Zhang, Z., Breidt, C., & Friedrich, K. (2005). Tribological properties of epoxy nanocomposites I. Enhancement of the wear resistance by nano-TiO<sub>2</sub> particles. *Wear*, *258*(1-4 SPEC. ISS.), 141–148. <https://doi.org/10.1016/j.wear.2004.09.005>

- Chindasiriphan, P., Yokota, H., & Pimpakan, P. (2020). Effect of fly ash and superabsorbent polymer on concrete self-healing ability. *Construction and Building Materials*, 233, 116975. <https://doi.org/10.1016/j.conbuildmat.2019.116975>
- Choudhury, S. K., & Chinchankar, S. (2017). Finish Machining of Hardened Steel. In *Comprehensive Materials Finishing* (Vols. 1–3). <https://doi.org/10.1016/B978-0-12-803581-8.09149-9>
- Chua Abdullah, M. I. H., Abdollah, M. F. Bin, Tamaldin, N., Amiruddin, H., & Nuri, N. R. M. (2016). Effect of hexagonal boron nitride nanoparticles as an additive on the extreme pressure properties of engine oil. *Industrial Lubrication and Tribology*, 68(4), 441–445. <https://doi.org/10.1108/ILT-10-2015-0157>
- Cortes, V., Sanchez, K., Gonzalez, R., Alcoutlabi, M., & Ortega, J. A. (2020). The Performance of SiO<sub>2</sub> and TiO<sub>2</sub> Nanoparticles as Lubricant Additives in Sunflower Oil. *Lubricants*, 8(1), 10. <https://doi.org/10.3390/lubricants8010010>
- Cui, Y., Ding, M., Sui, T., Zheng, W., Qiao, G., Yan, S., & Liu, X. (2020). Role of nanoparticle materials as water-based lubricant additives for ceramics. *Tribology International*, 142(July 2019), 105978. <https://doi.org/10.1016/j.triboint.2019.105978>
- Das, R. (2019). Eco-friendly lubricants for tribological application. *Handbook of Ecomaterials*, 5, 3269–3286. [https://doi.org/10.1007/978-3-319-68255-6\\_95](https://doi.org/10.1007/978-3-319-68255-6_95)
- Donnet, C., & Erdemir, A. (2006). Friction Mechanisms and Fundamental Aspects in Solid Lubricant Coatings. *Materials Surface Processing by Directed Energy Techniques*, 573–593. <https://doi.org/10.1016/B978-008044496-3/50018-6>
- Ebnesajjad, S., & Khaladkar, P. R. (2005). Properties of Neat (Unfilled) and Filled Fluoropolymers. *Fluoropolymers Applications in the Chemical Processing Industries*, 15–115. <https://doi.org/10.1016/b978-081551502-9.50006-5>
- Elsheikh, A. H., Yu, J., Sathyamurthy, R., Tawfik, M. M., Shanmugan, S., & Essa, F. A.

- (2020). Improving the tribological properties of AISI M50 steel using SnS/ZnO solid lubricants. *Journal of Alloys and Compounds*, 821. <https://doi.org/10.1016/j.jallcom.2019.153494>
- Ermakov, S. F. (2012). The effect of lubricants and additives on the tribological performance of solids. Part 1. Passive friction control. *Journal of Friction and Wear*, 33(1), 72–87. <https://doi.org/10.3103/S1068366612010059>
- Essa, F. A., Zhang, Q., & Huang, X. (2017). Investigation of the effects of mixtures of WS<sub>2</sub> and ZnO solid lubricants on the sliding friction and wear of M50 steel against silicon nitride at elevated temperatures. *Wear*, 374–375, 128–141. <https://doi.org/10.1016/j.wear.2017.01.098>
- Freyman, C., Zhao, B., & Chung, Y. W. (2007). Suppression of moisture sensitivity of friction in carbon-based coatings. *Superlubricity*, 295–310. <https://doi.org/10.1016/B978-044452772-1/50049-4>
- Gajrani, K. K., Suvin, P. S., Kailas, S. V., & Mamilla, R. S. (2019). Thermal, rheological, wettability and hard machining performance of MoS<sub>2</sub> and CaF<sub>2</sub> based minimum quantity hybrid nano-green cutting fluids. *Journal of Materials Processing Technology*, 266, 125–139. <https://doi.org/10.1016/j.jmatprotec.2018.10.036>
- Gamage, N., Liyanage, K., Fragomeni, S., & Setunge, S. (2011). Overview of Different Types of Fly Ash and Their Use As a Building and. *International Conference of Structure Engineering, Construction and Management, February*. Retrieved from <https://www.researchgate.net/publication/264707671>
- Gao, Y., Jiang, Y., Jiang, H., Zeng, S., Guo, F., & Li, J. (2019). Cholesterol ester derivatives as oil-based lubricant additives: Mesogenic and tribological properties. *Materials Research Express*, 6(12). <https://doi.org/10.1088/2053-1591/ab5564>
- Guo, X., & Zhang, T. (2020). Utilization of municipal solid waste incineration fly ash to produce autoclaved and modified wall blocks. *Journal of Cleaner Production*, 252, 119759. <https://doi.org/10.1016/j.jclepro.2019.119759>

- Guo, Z., Zhang, Y., Wang, J., Gao, C., Zhang, S., Zhang, P., & Zhang, Z. (2020). Interactions of Cu nanoparticles with conventional lubricant additives on tribological performance and some physicochemical properties of an ester base oil. *Tribology International*, 141(August 2019), 105941. <https://doi.org/10.1016/j.triboint.2019.105941>
- Guzman Borda, F. L., Ribeiro de Oliveira, S. J., Seabra Monteiro Lazaro, L. M., & Kalab Leiróz, A. J. (2018). Experimental investigation of the tribological behavior of lubricants with additive containing copper nanoparticles. *Tribology International*, 117, 52–58. <https://doi.org/10.1016/j.triboint.2017.08.012>
- Haseeb, A. S. M. A., Sia, S. Y., Fazal, M. A., & Masjuki, H. H. (2010). Effect of temperature on tribological properties of palm biodiesel. *Energy*, 35(3), 1460–1464. <https://doi.org/10.1016/j.energy.2009.12.001>
- Hongmei, X., Bin, J., Changping, T., Jiahong, D., Xin, Q., & Fusheng, P. (2019). Experimental evaluation of MoS<sub>2</sub> nanosheets as lubricant additive in different types of base oil for magnesium alloy/steel pairs. *Materials Research Express*, 6(6). <https://doi.org/10.1088/2053-1591/ab0fb8>
- Hower, J. C., Groppo, J. G., Graham, U. M., Ward, C. R., Kostova, I. J., Maroto-Valer, M. M., & Dai, S. (2017). Coal-derived unburned carbons in fly ash: A review. *International Journal of Coal Geology*, 179, 11–27. <https://doi.org/10.1016/j.coal.2017.05.007>
- Huang, X., Zhao, H., Hu, X., Liu, F., Wang, L., Zhao, X., Gao, P., & Ji, P. (2020). Optimization of preparation technology for modified coal fly ash and its adsorption properties for Cd<sup>2+</sup>. *Journal of Hazardous Materials*, 392(March), 122461. <https://doi.org/https://doi.org/10.1016/j.jhazmat.2020.122461>
- Jazaa, Y., & Chumbley, S. (2018). Effect of nanoparticle additives on the tribological behavior of oil under boundary lubrication. *Graduate Theses and Dissertations*. 1677322. Retrieved from <https://lib.dr.iastate.edu/etd/16773>
- Jiang, D., Li, X., Lv, Y., Zhou, M., He, C., Jiang, W., Liu, Z., & Li, C. (2020). Utilization



of limestone powder and fly ash in blended cement: Rheology, strength and hydration characteristics. *Construction and Building Materials*, 232, 117228. <https://doi.org/10.1016/j.conbuildmat.2019.117228>

Khan, M. S., Sisodia, M. S., Gupta, S., Feroskhan, M., Kannan, S., & Krishnasamy, K. (2019). Measurement of tribological properties of Cu and Ag blended coconut oil nanofluids for metal cutting. *Engineering Science and Technology, an International Journal*, 22(6), 1187–1192. <https://doi.org/10.1016/j.jestch.2019.04.005>

Kim, T., Ley, M. T., Kang, S., Davis, J. M., Kim, S., & Amrollahi, P. (2020). Using particle composition of fly ash to predict concrete strength and electrical resistivity. *Cement and Concrete Composites*, 107, 103493. <https://doi.org/10.1016/j.cemconcomp.2019.103493>

Kotia, A., Rajkhowa, P., Rao, G. S., & Ghosh, S. K. (2018). Thermophysical and tribological properties of nanolubricants: A review. *Heat and Mass Transfer/Waerme- Und Stoffuebertragung*, 54(11), 3493–3508. <https://doi.org/10.1007/s00231-018-2351-1>

Lentini, L., Moradi, M., & Colombo, F. (2018). A historical review of gas lubrication: From reynolds to active compensations. *Tribology in Industry*, 40(2), 165–182. <https://doi.org/10.24874/ti.2018.40.02.01>

Li, C., Li, M., Wang, X., Feng, W., Zhang, Q., Wu, B., & Hu, X. (2019). Novel carbon nanoparticles derived from biodiesel soot as lubricant additives. *Nanomaterials*, 9(8). <https://doi.org/10.3390/nano9081115>

Li, M., Zhang, J., Li, A., & Zhou, N. (2020). Reutilisation of coal gangue and fly ash as underground backfill materials for surface subsidence control. *Journal of Cleaner Production*, 254, 120113. <https://doi.org/10.1016/j.jclepro.2020.120113>

Liu, T., Zhou, C., Gao, C., Zhang, Y., Yang, G., Zhang, P., & Zhang, S. (2020). Preparation of Cu@SiO<sub>2</sub> composite nanoparticle and its tribological properties as water-based lubricant additive. *Lubrication Science*, 32(2), 69–79. <https://doi.org/10.1002/lc.1487>

- Matiliunaite, M., & Paulauskiene, T. (2019). From concept to practice: manufacturing of bio-lubricants from renewable resources. *Biomass Conversion and Biorefinery*, 9(2), 353–361. <https://doi.org/10.1007/s13399-018-0356-0>
- Maxwell, J. C. (1985). Chapter 5 Gases as Lubricating Fluids. *Tribology Series*, 9, 102-108. [https://doi.org/10.1016/50167-8922\(08\)70844-7](https://doi.org/10.1016/50167-8922(08)70844-7)
- Millán-Corrales, G., González-López, J. R., Palomo, A., & Fernandez-Jiménez, A. (2020). Replacing fly ash with limestone dust in hybrid cements. *Construction and Building Materials*, 243, 1–9. <https://doi.org/10.1016/j.conbuildmat.2020.118169>
- Mobili, A., Telesca, A., Marroccoli, M., & Tittarelli, F. (2020). Calcium sulfoaluminate and alkali-activated fly ash cements as alternative to Portland cement: study on chemical, physical-mechanical, and durability properties of mortars with the same strength class. *Construction and Building Materials*, 246, 118436. <https://doi.org/10.1016/j.conbuildmat.2020.118436>
- Mohanty, S., & Chugh, Y. P. (2007). Development of fly ash-based automotive brake lining. *Tribology International*, 40(7), 1217–1224. <https://doi.org/10.1016/j.triboint.2007.01.005>
- Mohd Khazani, A., Nur Riza, M. S., Nordin, J., Ahmad Samsuri, M., A. Rahim, A. T., & Mohd Faizal, Z. (2006). K-Chart: A Tool for Research Planning and Monitoring. *Journal of Quality Measurement and Analysis*, 2(1), 123–129. Retrieved from [https://www.academia.edu/2977536/K-Chart\\_a\\_tool\\_for\\_research\\_planning\\_and\\_monitoring](https://www.academia.edu/2977536/K-Chart_a_tool_for_research_planning_and_monitoring)
- Moreno, R. (2001). Rheology. In *Encyclopedia of Materials: Science and Technology* (Issue i, pp. 8192–8196). Elsevier. <https://doi.org/10.1016/B0-08-043152-6/01468-6>
- MS 816, (2007). Palm Olein - Specification (Second Revision). Malaysia: Department of Standards Malaysia.
- Mugahed Amran, Y. H., Soto, M. G., Alyousef, R., El-Zeadani, M., Alabduljabbar, H., &

- Aune, V. (2020). Performance investigation of high-proportion Saudi-fly-ash-based concrete. *Results in Engineering*, 6(February), 100118. <https://doi.org/10.1016/j.rineng.2020.100118>
- Nath, S. K. (2020). Fly ash and zinc slag blended geopolymer: Immobilization of hazardous materials and development of paving blocks. *Journal of Hazardous Materials*, 387, 121673. <https://doi.org/10.1016/j.jhazmat.2019.121673>
- Niraj, N., Pandey, K. M., & Dey, A. (2018). Tribological behaviour of Magnesium Metal Matrix Composites reinforced with fly ash cenosphere. *Materials Today: Proceedings*, 5(9), 20138–20144. <https://doi.org/10.1016/j.matpr.2018.06.382>
- Nosonovsky, M., Kailas, S. V, & Editors, M. R. L. (2013). Tribology for Scientists and Engineers. In P. L. Menezes, M. Nosonovsky, S. P. Ingole, S. V. Kailas, & M. R. Lovell (Eds.), *Tribology for Scientists and Engineers*. Springer New York. <https://doi.org/10.1007/978-1-4614-1945-7>
- O'Hara, R., Buchanan, F., & Dunne, N. (2014). Injectable calcium phosphate cements for spinal bone repair. In *Biomaterials for Bone Regeneration* (pp. 26–61). Elsevier. <https://doi.org/10.1533/9780857098104.1.26>
- Ogedengbe, T. S., Okediji, A. P., Yussouf, A. A., Aderoba, O. A., Abiola, O. A., Alabi, I. O., & Alonge, O. I. (2019). The Effects of Heat Generation on Cutting Tool and Machined Workpiece. *Journal of Physics: Conference Series*, 1378(2). <https://doi.org/10.1088/1742-6596/1378/2/022012>
- Paul, P. S., & Varadarajan, A. S. (2013). Performance evaluation of hard turning of AISI 4340 steel with minimal fluid application in the presence of semi-solid lubricants. *Proceedings of the Institution of Mechanical Engineers, Part J: Journal of Engineering Tribology*, 227(7), 738–748. <https://doi.org/10.1177/1350650112468376>
- Peña-Parás, L., Maldonado-Cortés, D., García, P., Irigoyen, M., Taha-Tijerina, J., & Guerra, J. (2017). Tribological performance of halloysite clay nanotubes as green lubricant additives. *Wear*, 376–377(May), 885–892. <https://doi.org/10.1016/j.wear.2017.01.044>

- Peng, D. X. (2015). Effects of concentration and temperature on tribological properties of biodiesel. *Advances in Mechanical Engineering*, 7(11), 1–10. <https://doi.org/10.1177/1687814015611025>
- Peng, D. X., Chen, C. H., Kang, Y., Chang, Y. P., & Chang, S. Y. (2010). Size effects of SiO<sub>2</sub> nanoparticles as oil additives on tribology of lubricant. *Industrial Lubrication and Tribology*, 62(2), 111–120. <https://doi.org/10.1108/00368791011025656>
- Peng, D. X., Kang, Y., Chen, S. K., & Chang, Y. P. (2010). Dispersion and tribological properties of liquid paraffin with added aluminum nanoparticles. *Industrial Lubrication and Tribology*, 62(6), 341–348. <https://doi.org/10.1108/00368791011076236>
- Purbasari, A., Ariyanti, D., & Sumardiono, S. (2020). Preparation and application of fly ash-based geopolymer for heavy metal removal. *AIP Conference Proceedings*, 2197(January), 1–6. <https://doi.org/10.1063/1.5140918>
- Rajendhran, N., Palanisamy, S., Periyasamy, P., & Venkatachalam, R. (2018). Enhancing of the tribological characteristics of the lubricant oils using Ni-promoted MoS<sub>2</sub> nanosheets as nano-additives. *Tribology International*, 118, 314–328. <https://doi.org/10.1016/j.triboint.2017.10.001>
- Ramanathan, S., Gopinath, S. C. B., Arshad, M. K. M., & Poopalan, P. (2020). Nanostructured aluminosilicate from fly ash: Potential approach in waste utilization for industrial and medical applications. *Journal of Cleaner Production*, 253. <https://doi.org/10.1016/j.jclepro.2019.119923>
- Rawat, S. S., Harsha, A. P., Das, S., & Deepak, A. P. (2020). Effect of CuO and ZnO Nano-Additives on the Tribological Performance of Paraffin Oil–Based Lithium Grease. *Tribology Transactions*, 63(1), 90–100. <https://doi.org/10.1080/10402004.2019.1664684>
- Ren, B., Gao, L., BotaoXie, Li, M., Zhang, S., Zu, G., & Ran, X. (2020). Tribological properties and anti-wear mechanism of ZnO@graphene core-shell nanoparticles as

- lubricant additives. *Tribology International*, 144(October 2019), 106114. <https://doi.org/10.1016/j.triboint.2019.106114>
- Salah, N., Abdel-wahab, M. S., Alshahrie, A., Alharbi, N. D., & Khan, Z. H. (2017). Carbon nanotubes of oil fly ash as lubricant additives for different base oils and their tribology performance. *RSC Advances*, 7(64), 40295–40302. <https://doi.org/10.1039/C7RA07155H>
- Salah, N., Abdel-wahab, M. S., Habib, S. S., & Khan, Z. H. (2017). Lubricant Additives Based on Carbon Nanotubes Produced from Carbon-Rich Fly Ash. *Tribology Transactions*, 60(1), 166–175. <https://doi.org/10.1080/10402004.2016.1155784>
- Salah, N., Alshahrie, A., Alharbi, N. D., Abdel-wahab, M. S., & Khan, Z. H. (2019). Nano and micro structures produced from carbon rich fly ash as effective lubricant additives for 150SN base oil. *Journal of Materials Research and Technology*, 8(1), 250–258. <https://doi.org/10.1016/j.jmrt.2017.12.003>
- Shaikh, V. A., & Boubekri, N. (2020). Using Vegetable-Oil-Based Sustainable Metal Working Fluids to Promote Green Manufacturing. *International Journal of Manufacturing, Materials, and Mechanical Engineering*, 10(1), 1–19. <https://doi.org/10.4018/IJMMME.2020010101>
- Singh, N., Singh, Y., Sharma, A., & Singla, A. (2019). Effect of addition of copper nanoparticles on the tribological behavior of macadamia oil at different sliding speeds. *Energy Sources, Part A: Recovery, Utilization, and Environmental Effects*, 41(23), 2917–2928. <https://doi.org/10.1080/15567036.2019.1582734>
- Straffelini, G. (2015). Wear mechanisms. *Springer Tracts in Mechanical Engineering*, 11, 85–113. [https://doi.org/10.1007/978-3-319-05894-8\\_4](https://doi.org/10.1007/978-3-319-05894-8_4)
- Struble, L. J., & Ji, X. (2001). Rheology. In *Handbook of Analytical Techniques in Concrete Science and Technology* (pp. 333–367). Elsevier. <https://doi.org/10.1016/B978-081551437-4.50012-6>

- Sulima, I., Klimczyk, P., & Malczewski, P. (2014). Effect of TiB<sub>2</sub> Particles on the Tribological Properties of Stainless Steel Matrix Composites. Retrieved from [https://www.amse.org.cn/article/2014/1006-7191-27-1-12/40195\\_2013\\_2\\_Fig1\\_HTML.gif.html](https://www.amse.org.cn/article/2014/1006-7191-27-1-12/40195_2013_2_Fig1_HTML.gif.html)
- Suresh Kumar Mandru et al., Suresh Kumar Mandru et al. (2019). A Review of an Effect of Canola Oil Lubrication with Nano Molybdenum Disulphide Additives on Machining. *International Journal of Mechanical and Production Engineering Research and Development*, 9(4), 761–768. <https://doi.org/10.24247/ijmperdaug201976>
- Suresha, B., Hemanth, G., Rakesh, A., & Adarsh, K. M. (2020). Tribological Behaviour of Neem Oil with and without Graphene Nanoplatelets Using Four-Ball Tester. *Advances in Tribology*, 2020, 1–11. <https://doi.org/10.1155/2020/1984931>
- Syahir, A. Z., Zulkifli, N. W. M., Masjuki, H. H., Kalam, M. A., Alabdulkarem, A., Gulzar, M., Khuong, L. S., & Harith, M. H. (2017). A review on bio-based lubricants and their applications. *Journal of Cleaner Production*, 168, 997–1016. <https://doi.org/10.1016/j.jclepro.2017.09.106>
- Talib, N., Nasir, R. M., & Rahim, E. A. (2017). Tribological behaviour of modified jatropa oil by mixing hexagonal boron nitride nanoparticles as a bio-based lubricant for machining processes. *Journal of Cleaner Production*, 147, 360–378. <https://doi.org/10.1016/j.jclepro.2017.01.086>
- Tang, Z., & Li, S. (2014). A review of recent developments of friction modifiers for liquid lubricants (2007-present). *Current Opinion in Solid State and Materials Science*, 18(3), 119–139. <https://doi.org/10.1016/j.cossms.2014.02.002>
- Verma, V., Tewari, P. C., Ahamed, R. Z., & Ahmed, S. T. (2019). Effect of Addition of Fly ash and Al<sub>2</sub>O<sub>3</sub> Particles on Mechanical and Tribological Behavior of Al MMC at Varying Load, Time and Speed. *Procedia Structural Integrity*, 14(2018), 68–77. <https://doi.org/10.1016/j.prostr.2019.05.010>
- Wang, J., Shi, Q., Huang, Z., Gu, Y., Musango, L., & Yang, Y. (2015). Experimental

- Investigation of Particle Size Effect on Agglomeration Behaviors in Gas-Solid Fluidized Beds. *Industrial and Engineering Chemistry Research*, 54(48), 12177–12186. <https://doi.org/10.1021/acs.iecr.5b02548>
- Wang, L., Wu, H., Zhang, D., Dong, G., Xu, X., & Xie, Y. (2018). Synthesis of a novel borate ester containing a phenylboronic group and its tribological properties as an additive in PAO 6 base oil. *Tribology International*, 121(February), 21–29. <https://doi.org/10.1016/j.triboint.2018.01.033>
- Wang, Y., Liu, C., Tan, Y., Wang, Y., & Li, Q. (2020). Chloride binding capacity of green concrete mixed with fly ash or coal gangue in the marine environment. *Construction and Building Materials*, 242, 118006. <https://doi.org/10.1016/j.conbuildmat.2020.118006>
- Wang, Y., Tan, Y., Wang, Y., & Liu, C. (2020). Mechanical properties and chloride permeability of green concrete mixed with fly ash and coal gangue. *Construction and Building Materials*, 233, 117166. <https://doi.org/10.1016/j.conbuildmat.2019.117166>
- Werth, J. ., Linsenbühler, M., Dammer, S. ., Farkas, Z., Hinrichsen, H., Wirth, K.-E., & Wolf, D. . (2003). Agglomeration of charged nanopowders in suspensions. *Powder Technology*, 133(1–3), 106–112. [https://doi.org/10.1016/S0032-5910\(03\)00096-2](https://doi.org/10.1016/S0032-5910(03)00096-2)
- Wu, H., Zhao, J., Xia, W., Cheng, X., He, A., Yun, J. H., Wang, L., Huang, H., Jiao, S., Huang, L., Zhang, S., & Jiang, Z. (2017). A study of the tribological behaviour of TiO<sub>2</sub> nano-additive water-based lubricants. *Tribology International*, 109, 398–408. <https://doi.org/10.1016/j.triboint.2017.01.013>
- Xie, H., Dang, S., Jiang, B., Xiang, L., Zhou, S., Sheng, H., Yang, T., & Pan, F. (2019). Tribological performances of SiO<sub>2</sub>/graphene combinations as water-based lubricant additives for magnesium alloy rolling. *Applied Surface Science*, 475(January), 847–856. <https://doi.org/10.1016/j.apsusc.2019.01.062>
- Xie, H., Jiang, B., He, J., Xia, X., & Pan, F. (2016). Lubrication performance of MoS<sub>2</sub> and SiO<sub>2</sub> nanoparticles as lubricant additives in magnesium alloy-steel contacts. *Tribology*

*International*, 93, 63–70. <https://doi.org/10.1016/j.triboint.2015.08.009>

Xing, Y., Guo, F., Xu, M., Gui, X., Li, H., Li, G., Xia, Y., & Han, H. (2019). Separation of unburned carbon from coal fly ash: A review. *Powder Technology*, 353, 372–384. <https://doi.org/10.1016/j.powtec.2019.05.037>

Yadav, G., Tiwari, S., & Jain, M. L. (2018). Tribological analysis of extreme pressure and anti-wear properties of engine lubricating oil using four ball tester. *Materials Today: Proceedings*, 5(1), 248–253. <https://doi.org/10.1016/j.matpr.2017.11.079>

Ye, J., Burris, D. L., & Xie, T. (2016). A review of transfer films and their role in ultra-low-wear sliding of polymers. *Lubricants*, 4(1), 1–15. <https://doi.org/10.3390/lubricants4010004>

Yunus, R., & Luo, X. (2017). Thermochemical Conversion of Plant Oils and Derivatives to Lubricants. In *Advances in Bioenergy* (Vol. 2). Elsevier Ltd. <https://doi.org/10.1016/bs.aibe.2016.11.001>

Zhang, D., Yang, Q., Mao, M., & Li, J. (2020). Carbonation performance of concrete with fly ash as fine aggregate after stress damage and high temperature exposure. *Construction and Building Materials*, 242, 118125. <https://doi.org/10.1016/j.conbuildmat.2020.118125>

Zhang, H. (2016). Surface Characterization Techniques for Polyurethane Biomaterials. In *Advances in Polyurethane Biomaterials*. Elsevier Ltd. <https://doi.org/10.1016/B978-0-08-100614-6.00002-0>

Zhang, L., Yang, F., & Tao, Y. (2020). Removal of unburned carbon from fly ash using enhanced gravity separation and the comparison with froth flotation. *Fuel*, 259(March 2019), 116282. <https://doi.org/10.1016/j.fuel.2019.116282>

Zhang, N., Yu, H., Gong, W., Liu, T., Wang, N., Tan, Y., & Wu, C. (2020). Effects of low- and high-calcium fly ash on the water resistance of magnesium oxysulfate cement. *Construction and Building Materials*, 230, 116951.



<https://doi.org/10.1016/j.conbuildmat.2019.116951>

Zhao, Y., Yu, M., Xiang, Y., Kong, F., & Li, L. (2020). A sustainability comparison between green concretes and traditional concrete using an energy ternary diagram. *Journal of Cleaner Production*, 256. <https://doi.org/10.1016/j.jclepro.2020.120421>

Zhou, K., Gong, K., Zhou, Q., Zhao, S., Guo, H., & Qian, X. (2020). Estimating the feasibility of using industrial solid wastes as raw material for polyurethane composites with low fire hazards. *Journal of Cleaner Production*, 257. <https://doi.org/10.1016/j.jclepro.2020.120606>

